J_ID: Z3Q Customer A_ID: 04-1248 Cadmus Art: IJC5519 Date: 22-FEBRUARY-05 Stage: I

TABLE II – CHEMOSENSITIVITY TO PROTEIN KINASE INHIBITORS[1]

Inhibitor	Target	IC_{50} values (μM)		RR[2]
		PC-9	PC-9/ZD	
AG-1478	EGFR	0.052 ± 0.02	6.0 ± 0.8	117
RG-14620	EGFR	13 ± 1.0	13 ± 2.5	1.0
Lavendustin A	EGFR	20 ± 4.6	27 ± 2.6	1.3
Genistein	TK	18 ± 1.5	27 ± 1.5	1.5
K252a	PKC	0.47 ± 0.17	0.63 ± 0.04	1.3
Staurosporin	PKC	0.0036 ± 0.0019	0.004 ± 0.0014	1.1
AG-825	HER2	>50	>50	

[1]Assessed by MTT assay in PC-9 and PC-9/ZD cells. Values are the mean ± SD of >3 independent experiments.–[2]Relative resistance value (IC_{50} of resistant cells/IC_{50} of parental cells).

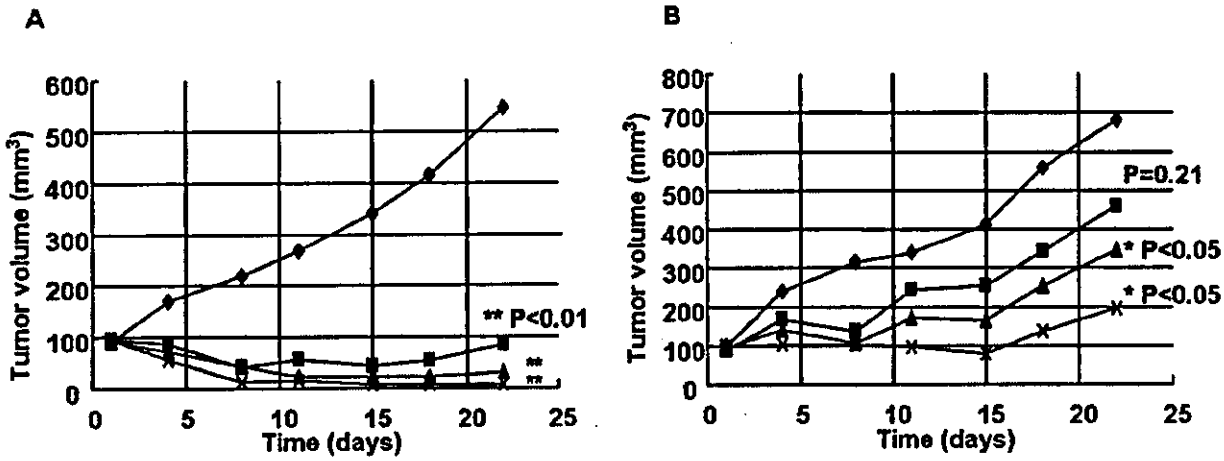

FIGURE 2 - Growth-inhibitory effect of gefitinib on PC-9 and PC-9/ZD cells xenotransplanted into nude mice. Ten days before gefitinib administration, 5×10^6 PC-9 (*a*) or PC-9/ZD (*b*) cells were injected s.c. into the back of mice. The mice were divided into 4 groups (◆, control group; ■, 12.5 mg/Kg group; ▲, 25 mg/Kg group; ×, 50 mg/Kg group). Gefitinib was administered p.o. to the tumor-inoculated mice on Days 1–21. Each group consisted of 6 mice. The statistical analysis was carried out by using the unpaired *t*-test.

ATP-binding site of the Bcr-Abl, the target of the drug.[21,27] We analyzed the sequences of the cDNAs of EGFR, HER2, and HER3, but found no differences in their sequences between PC-9 and PC-9/ZD cells. We did detect a deleted position of EGFR in both cell lines that results in deletion of 5 amino acids (Glu722, Leu723, Arg724, Glu725, and Ala726) (Fig. 4). Our findings indicate that the deletion does not directly contribute to the cellular resistance.

F4

Inhibitory effect of gefitinib on autophosphorylation of EGFR in PC-9/ZD cells

Phosphorylation of EGFR is necessary for EGFR-mediated intracellular signaling. Although the EGFR phosphorylation levels of tumors were thought to be correlated with sensitivity to gefitinib, the basal level of phosphorylated EGFR in PC-9 and PC-9/ZD cells is almost the same. Gefitinib inhibited EGFR autophosphorylation in a dose-dependent manner and completely inhibited its phosphorylation at 0.2–2 μM in PC-9 cells (Fig. 5*a*), but its inhibitory effect on autophosphorylation of EGFR in PC-9/ZD cells was less than in PC-9 cells (Fig. 5*a*). Because each phosphorylation site of EGFR has a different role in the activation of downstream signaling molecules, we examined the inhibitory effect of gefitinib on site-specific phosphorylation of EGFR. Phosphorylation of several different EGFR tyrosine residues (Tyr845, Tyr992 and Tyr1068) was dose-dependently inhibited by gefitinib in PC-9 cells, whereas no clear inhibitory effects of gefitinib on phosphorylation at Tyr 845 and Tyr1068 residues in PC-9/ZD cells was observed (Fig. 5*b,c,e*). The most marked difference of in inhibition between the cells was observed at Tyr1068 (Fig. 5*e*). Tyr1045 showed resistance to inhibition of autophosphorylation by gefitinib in both PC-9 and PC-9/ZD cells (Fig. 5*d*).

F5

Complex formation of EGFR and its adaptor proteins

Tyr1068 of EGFR is the tyrosine that is most resistant to inhibition of autophosphorylation by gefitinib in PC-9/ZD cells. Because the Tyr 1068 is a direct binding site for the Grb2/SH2 domain, and its phosphorylation is related to the complex formation of EGFR-adaptor proteins and their signaling, we examined complex formation between EGFR and the adaptor proteins GRB2, SOS, Shc, and PI3K by immunoprecipitation. The level of expression of these proteins in PC-9 and PC-9/ZD cells were similar (Fig. 3*a*). A smaller amount of EGFR-GRB2 complex was observed in PC-9/ZD cells and no EGFR-SOS complex was detected at all (Fig. 6). The amount of HER2- or HER3-GRB2 complex in PC-9 and PC-9/ZD cells was similar, and no decreases in complex formation were observed after exposure to gefitinib. A decreased amount of HER2-SOS complex and inability to detect HER3-SOS complex were also observed in PC-9/ZD cells. HER2-PI3K complex increased in PC-9/ZD. There are no significant differences in complex formation between SHC and EGFR, HER2, or HER3 between PC-9 and PC-9/ZD cells. These results suggest that Grb2-SOS-mediated signaling may be inactivated in PC-9/ZD cells.

F6

Heterodimerization of HER family member in PC-9/ZD cells

Dimerization of members of the HER family is essential for activation of their catalytic activity and their signaling. We examined the effect of gefitinib on the dimerization of HER family members by immunoblotting, immunoprecipitation and chemical cross-linking analysis (Figs. 3*a*, 5*a*, 7*a*). The expression levels of EGFR and HER2 were similar and the HER3 level was lower in PC-9/ZD cells by immunoblotting (Fig. 3*a*). A chemical cross-

F7

J_ID: Z3Q Customer A_ID: 04-1248 Cadmus Art: IJC5519 Date: 22-FEBRUARY-05 Stage: I

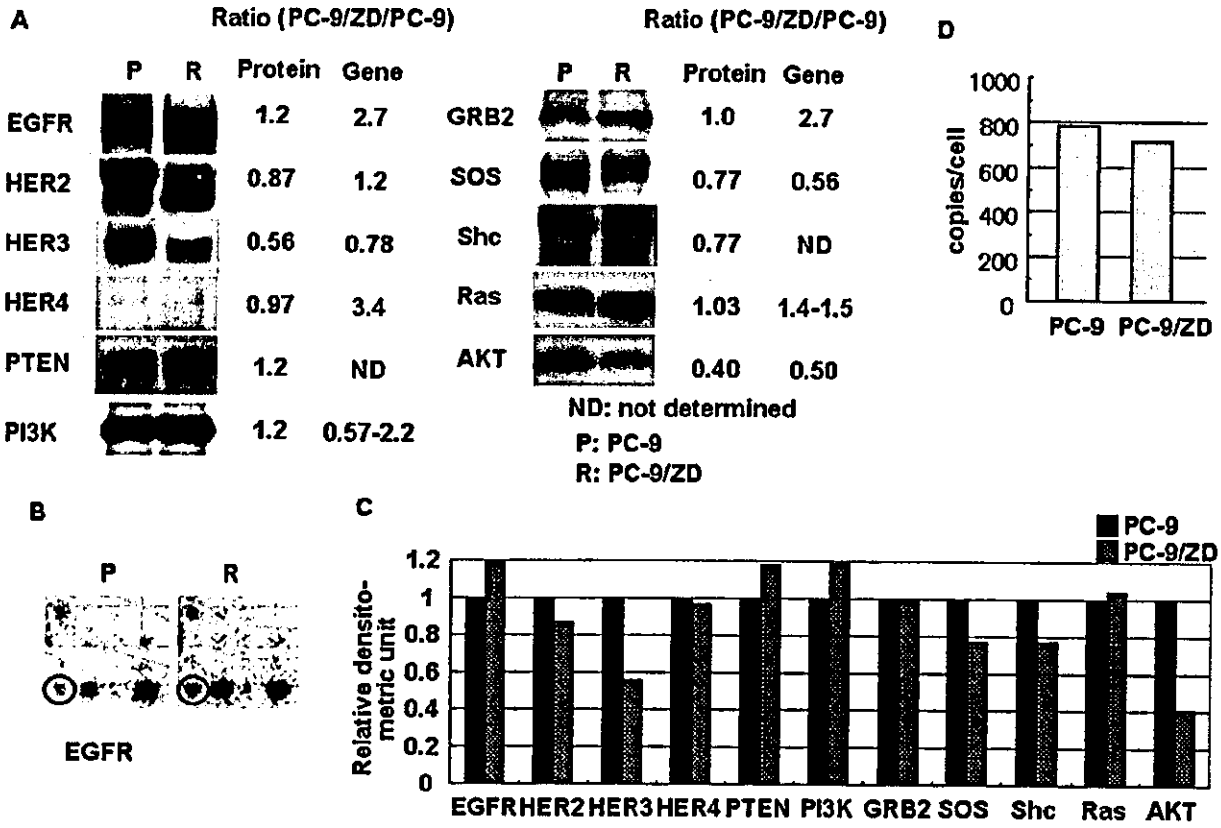

FIGURE 3 – Expresssion of HER family members and related molecules in PC-9 (P) and PC-9/ZD (R) cells. (*a*) Western blot analysis; a 20 μg sample of total cell lysates was separated by SDS-PAGE, transferred to a PVDF membrane, and incubated with a specific anti-human antibody as the first antibody and then with horseradish peroxidase-conjugated secondary antibody. The ratios of the levels of expression of proteins and genes in PC-9 cells to the levels in PC-9/ZD cells are shown. (*b*) cDNA expression array; Poly A RNA was converted into ^{32}P-labeled first-strand cDNA with MMLV reverse transcriptase. The ^{32}P-labeled cDNA fraction was hybridized to the membrane on which fragments of 777 genes were spotted. The close-up view shows EGFR mRNA expression. (*c*) Each band was quantified by a densitometry and with NIH image software. The levels of protein expression are shown in a graph. (*d*) Absolute amounts of EGFR transcripts of PC-9 cells and PC-9/ZD cells measured by real-time quantitative RT-PCR. The values were calculated back to the initial cell numbers for RNA extraction in Material and Methods.

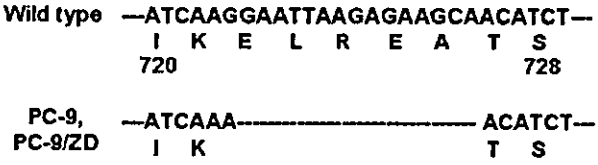

FIGURE 4 – Detection of a deleted position of EGFR. Direct sequencing of a PC-9 and PC-9/ZD-derived, amplified cDNA fragment containing the ATP-binding site of EGFR. *Top*, wild-type EGFR; *bottom*, PC-9 and PC-9/ZD.

linking assay showed that in the absence of gefitinib the amount of high molecular weight complexes (~400 kDa) that are recognized by anti-EGFR antibody (EGFR dimers), including formations of homodimers and heterodimers (EGFR-EGFR, EGFR-HER2 or EGFR-HER3), was almost the same in PC-9 and PC-9/ZD cells, whereas HER2 dimerization detected by anti-HER2 antibody was remarkably lower in PC-9/ZD cells (Fig. 7*a*). Increased EGFR/HER2 (and EGFR/HER3) heterodimer formation was detected in PC-9/ZD cells by immunoprecipitation analysis (Fig. 5*a*). The proportion of EGFR heterodimer to homodimer is increased significantly in PC-9/ZD (Fig. 7*b*). When exposed to gefitinib at a concentration of 0.2 μM for 6 hr the amount of dimer-formation increased similarly in PC-9 and PC-9/ZD cells (Fig. 7*a*), whereas marked induction of hetero-dimerization of EGFR-HER2 was observed only in PC-9 cells (Fig. 5*a*). These results suggest that a difference in hetero- or homo-dimerization is a possible determinant factor of gefitinib sensitivity.

AKT and MAPK pathways in PC-9/ZD cells

Because phosphorylation at Tyr 1068 of EGFR plays an important role for transduction of the signal to downstream of MAPK and AKT pathway,[28,29] we examined the difference between PC-9 and PC-9/ZD cells in downstream signaling. The basal level of phosphorylated AKT is higher in PC-9 cells than in PC-9/ZD cells, and although gefitinib inhibited AKT phosphorylation in a dose-dependent manner (Fig. 9*a*), the inhibitory effect of gefitinib on phosphorylation of AKT in PC-9/ZD cells was significantly less than in PC-9 cells (Fig. 9*a*). This difference in the inhibitory effect of gefitinib on AKT phosphorylation between PC-9 and PC-9/ZD cells is very similar to the difference in effect on EGFR autophosphorylation. No inhibition of phosphorylation of MAPK by gefitinib was observed in either cell line (Fig. 9*b*). These results suggest that downregulation of activated AKT is closely correlated with the cellular sensitivity to gefitinib, but that inhibition of the MAPK pathway does not contribute to drug sensitivity. AQ4

J_ID: Z3Q Customer A_ID: 04-1248 Cadmus Art: IJC5519 Date: 22-FEBRUARY-05 Stage: I

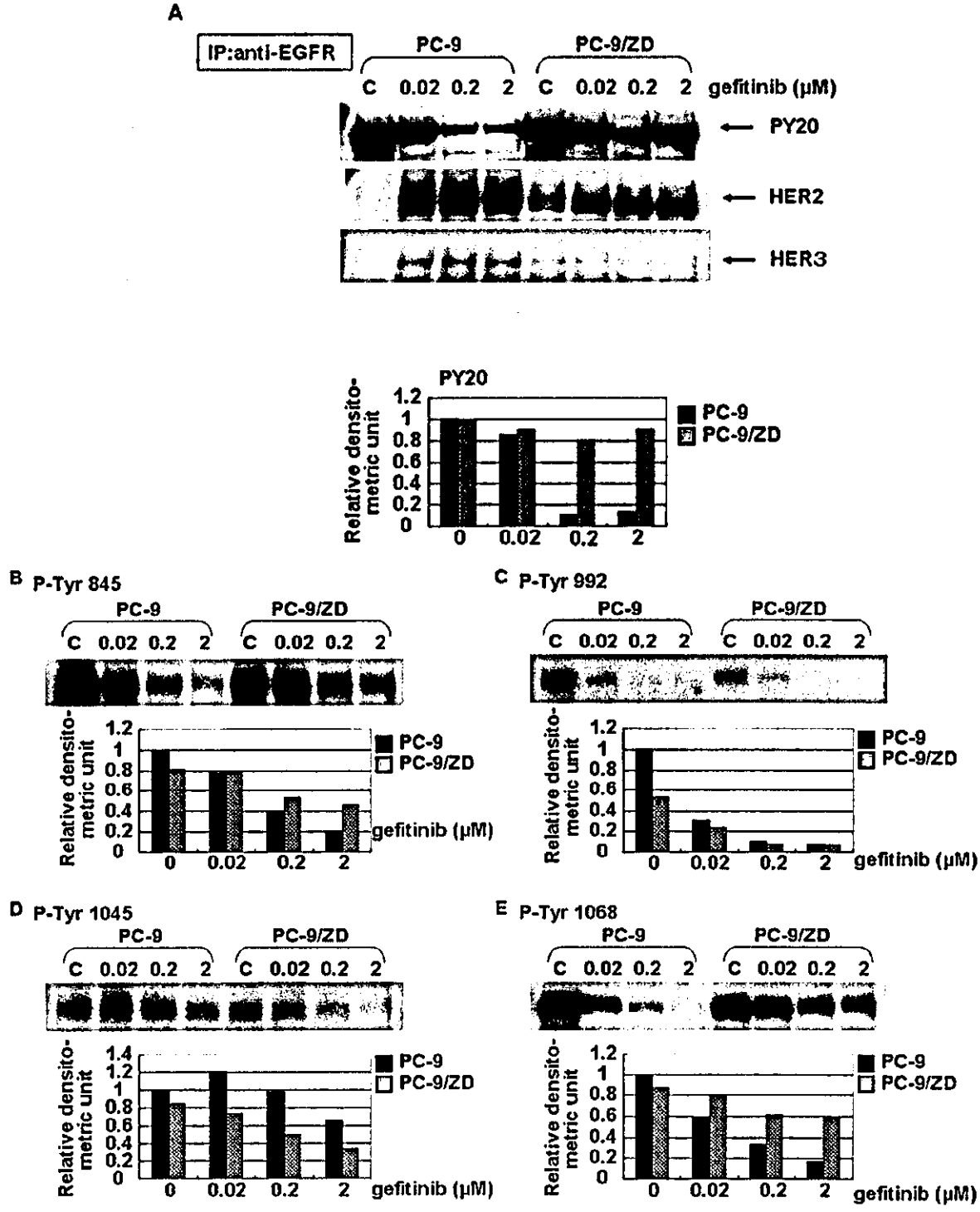

FIG. 5 – Effect of gefitinib on autophosphorylation of EGFR. (*a*) PC-9 and PC-9/ZD cells (5×10^6) were exposed to 0.02, 0.2 or 2 μM gefitinib for 6 hr. The 1,500 μg of total cell lysate was immunoprecipitated with an anti EGFR antibody. The immunoprecipitates were subjected to gel electrophoresis and Western blotting with anti-phosphotyrosine, anti-HER2 and anti-HER3 antibodies. Tyrosine-phosphorylated EGFR was determined with an anti-phosphotyrosine antibody. Heterodimer formation of EGFR was analyzed with anti-HER2 and anti-HER3 antibodies. The expression levels have been plotted in a graph. (*b–e*) PC-9 and PC-9/ZD cells were exposed to 0.02, 0.2 and 2 μM gefitinib for 6 hr. A 20 μg of protein of each sample was analyzed by Western blotting by using anti phospho-EGFR (Tyr845, Tyr992, Tyr 1045, Tyr 1068) antibodies.

J_ID: Z3Q Customer A_ID: 04-1248 Cadmus Art: IJC5519 Date: 22-FEBRUARY-05 Stage: I

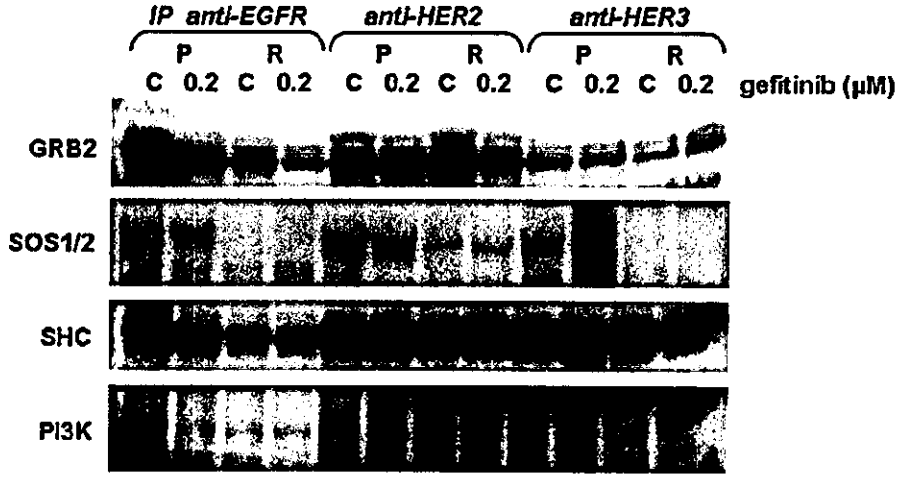

FIGURE 6 – Protein interaction between EGFR and its adaptor proteins. Cells (P: PC-9, R: PC-9/ZD) were exposed to 0 and 0.2 μM of gefitinib for 6 hr. The cells were lysed and immunoprecipitated with ant-EGFR, anti-HER2, and anti-HER3 antibodies, and the amounts of the Grb2, SOS1/2, SHC and PI3K precipitated were monitored by immunoblotting with their specific Abs.

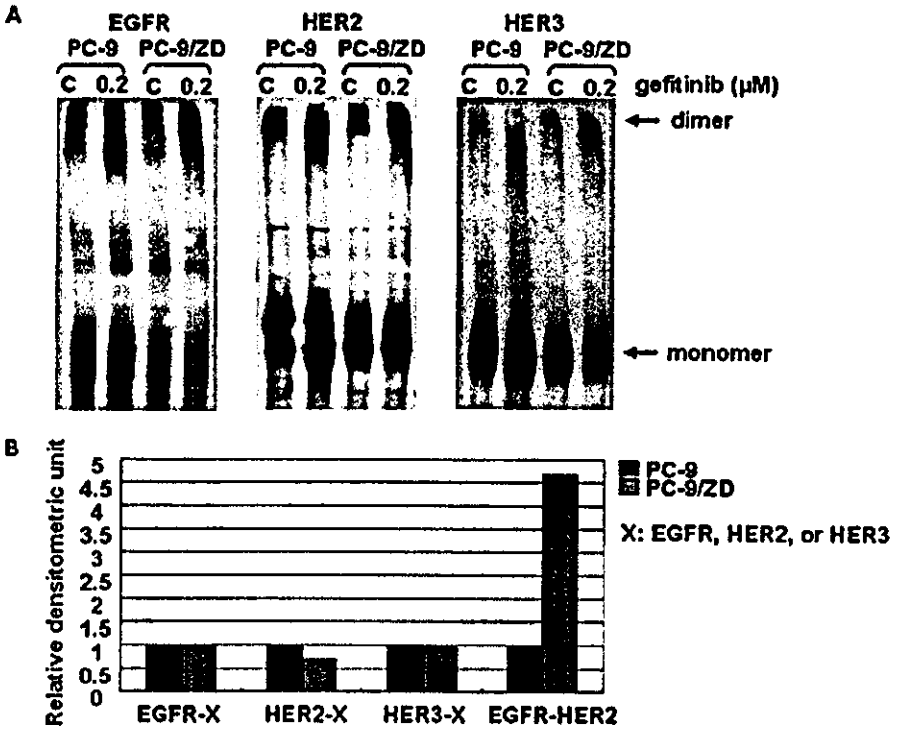

FIGURE 7 – Chemical cross-linking of PC-9 and PC-9/ZD cells. (*a*) After 6 hr exposure to 1.5 mM bis (sulfosuccinimidyl) substrate dissolved in PBS as indicated in Material and Methods. The cross-linking reaction was quenched and the cell lysates were prepared and subjected to immunoblot analysis of EGFR, HER2 and HER3. (*b*) Ratio of dimmers formed by PC-9 cells to those by PC-9/ZD cells in the absence of gefitinib. The density of the bands in (*a*) for EGFR-X, HER2-X and HER3-X were quantified densitometrically. The ratio of EGFR-HER2 was calculated by the band density obtained in Figure 5*a*. X = EGFR, HER2 or HER3.

Discussion

Interest in resistance to target-based therapy (TBT) has been growing ever since clinical efficacy was first demonstrated.[11–13] Although CML patients respond to STI-571 well at first, most patients eventually relapse in the late stage of the disease.[25–27] It has been reported that some patients in whom treatment with gefitinib is effective at first, ultimately become refractory.[30] Resistance is likely to remain a hurdle that limits the long-term effectiveness of TBT. PC-9 had a deletion mutation within the kinase domain of EGFR and is highly sensitive. These characters are similar to those of NSCLC with clinical responsiveness to gefitinib. Analyzing the mechanism of resistance of PC-9/ZD subline might be clinically meaningful.

The mechanism of drug resistance is thought to be multifactorial. Because the growth-inhibitory assay in our present study showed no cross resistance to a variety of cytotoxic agents, the mechanism of the resistance differs from the mechanism of multidrug resistance patterns. Although expression of BCRP, one of the multidrug-resistance-related proteins has been reported to contribute to the resistance to gefitinib,[31] expression of BCRP mRNA is observed only in PC-9 cells (data not shown). Although mutations in the ATP-binding pocket of BCR-ABL gene have been identified recently in cells from CML patients who were refractory to STI-571 treatment or relapse,[25–27] there have been no reports of any such mutations for gefitinib resistance. PC-9/ZD also became refractory to gefitinib without secondary mutation in EGFR cDNA. These suggest the possibility of refractory tumor after treatment of gefitinib including this kind of phenotype.

There is no significant difference in expression level of EGFR between PC-9 and PC-9/ZD. Does the antitumor effect of gefitinib

J_ID: Z3Q Customer A_ID: 04-1248 Cadmus Art: IJC5519 Date: 22-FEBRUARY-05 Stage: I

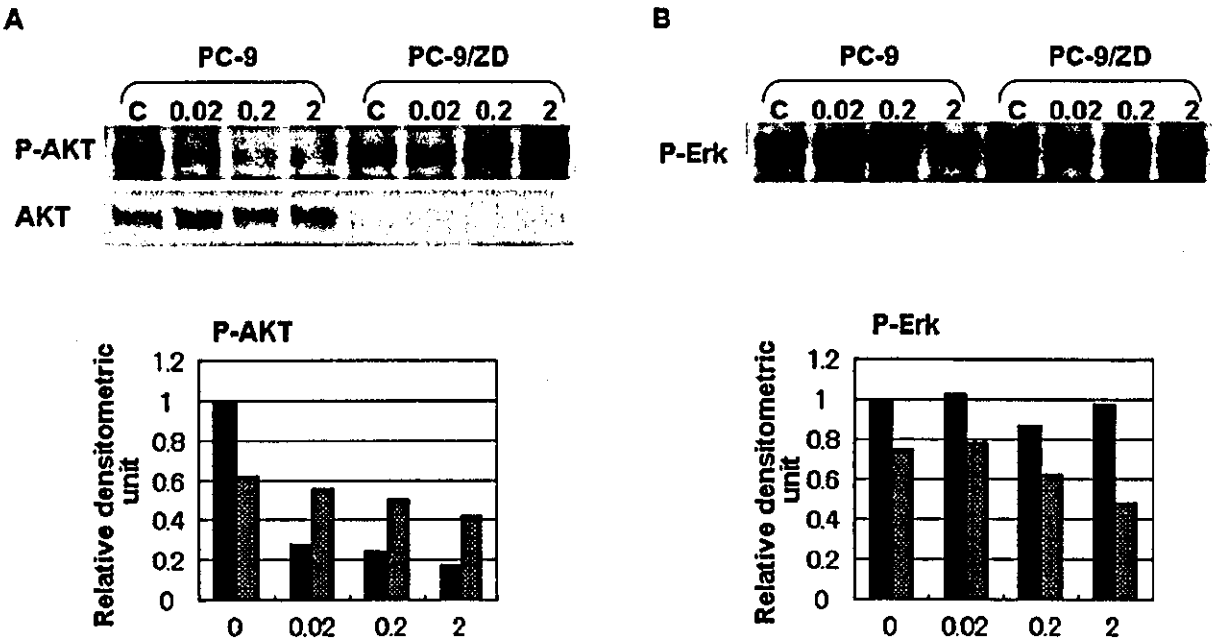

FIGURE 8 · Effect of gefitinib on the MAPK and AKT pathway. Cells were placed in medium containing 0, 0.02, 0.2 or 2 μM of gefitinib for 6 hr and harvested in EBC buffer. Total cellular lysates were separated on SDS-PAGE, transferred to a membrane and blotted with (*a*) anti-phospho-AKT (Ser473) and (*b*) anti-phospho-Erk (p44/42) antibodies. The expression levels are shown in a graph.

require EGFR expression? Naruse *et al.*[32] suggested that the high sensitivity of K562/TPA to gefitinib is due to acquired EGFR expression. In their study autophosphorylation of EGFR in K562/TPA cells was inhibited by 0.01 μM gefitinib, and the IC_{50}-value of gefitinib in parental K562 cells, which do not express EGFR, was approximately 400-fold higher than that in the K562/TPA subline. Furthermore, most patients who responded to gefitinib therapy have EGFR mutation in lung tumor.[18,19] These findings suggest strongly that gefitinib exerts its antitumor effect through an action on EGFR. Our present study showed similar EGFR expression and autophosphorylation levels in PC-9 and PC-9/ZD cells. The inhibitory effect of gefitinib on phosphorylation of EGFR is different. PC-9/ZD did not show cross-resistance to the specific EGFR TK inhibitors RG-14620 and Lavendustin A in an MTT assay, nor did inhibit the phosphorylation of EGFR at the cellular level (data not shown). Paez *et al.*[18] reported that phosphorylation of EGFR in gefitinib-resistant cell lines was inhibited only when gefitinib was present at high concentration. These findings suggest that the difference in the inhibitory-effect on EGFR phosphorylation may determine the efficacy of the drug.

The inhibitory effect of gefitinib on EGFR phosphorylation is not significant in PC-9/ZD cells despite the absence of differences in the sequences of EGFR, HER2, and HER3. There are several possible explanations for the difference in inhibitory effect. First, the avidity of gefitinib for the ATP-binding site of EGFR may be decreased in PC-9/ZD cells due to a protein-protein interaction, *i.e.*, EGFR and a certain protein prevent gefitinib from binding to EGFR. Second, a change in the activity of specific protein-tyrosine kinase or phosphatase of EGFR in PC-9/ZD cells, especially after exposure to gefitinib, may result in resistance to inhibition of EGFR phosphorylation. The phosphorylation level is maintained in exquisite balance by the reciprocal activities of kinase and phosphatase,[33,34] and Wu reported that phosphatase plays a role in STI571-resistance.[35] Third, increased heterodimer formation by EGFR with other members of the HER family results in the limited inhibition. Heterodimer formation is increased in PC-9/ZD cells under basal conditions, and no increase in formation was observed after exposure to gefitinib, although marked heterodimer induction was observed in PC-9 cells. Calculations in *in vitro* studies have shown that the IC_{50}-value for inhibition of the tyrosine kinase activity of EGFR is 0.023–0.079 μM, whereas the IC_{50}-value for inhibition of HER2 is 100-fold higher.[36] We estimate that the inhibitory effect of gefitinib depends on the ratio of homodimer formation to heterodimer formation, and the heterodimer may be one of the routes of escape from the action of gefitinib.

Signal transduction by the HER family member is mediated by 2 major pathways, the MAPK signaling pathway and the AKT signaling pathway, which regulate cell proliferation and survival. Because phosphorylated AKT was inhibited completely by gefitinib in PC-9 cells, but inhibition of phosphorylated MAPK was not significant, inhibition of the AKT pathway may be more important to cell sensitivity than inhibition of MAPK. Moasser *et al.*[37] reported consistent results, showing that downregulation of AKT activity is predominantly seen in tumors that are sensitive to gefitinib. The phosphorylation of AKT and MAPK was not inhibited significantly by gefitinib in PC-9/ZD cells. This finding might be attributable to inactivation of Tyr 1068-Grb2-SOS-mediated signaling.

Based on the results of this comparative study, EGFR-Grb2-SOS complex formation, phosphorylation of Tyr1068, the ratio of the amount of homodimer formation to heterodimer formation, and the AKT signaling pathway are possible predictive biomarkers for gefitinib sensitivity. As a different approach, we are now looking for the genes associated with gefitinib resistance in PC-9/ZD cells compared to PC-9 cells by subtractive cloning.

Acknowledgements

"Iressa" is a trademark of the AstraZeneca group of companies.

J_ID: Z3Q Customer A_ID: 04-1248 Cadmus Art: IJC5519 Date: 22-FEBRUARY-05 Stage: I

References

1. Socinski MA. Addressing the optimal duration of therapy in advanced, metastatic non-small-cell lung cancer. Am Soc Clin Oncol 2003;144–52.
2. Nicholson RI, Gee JM, Harper ME. EGFR and cancer prognosis. Eur J Cancer 2001;37:S9–15.
3. Mendelsohn J, Baselga J. The EGF receptor family as targets for cancer therapy. Oncogene 2000;19:6550–65.
4. Salmon DS, Brandt R, Ciardiello F, Normanno N. Epidermal growth factor-related peptides and their receptors in human malignancies. Crit Rev Oncol Hematol 1995;19:182–232.
5. Fox SB, Smith K, Hollyer J, Greenall M, Hastrich D, Harris AL. The epidermal growth factor receptor as a prognostic marker: result of 370 patients and review of 3009 patients. Breast Cancer Res Treat 1994;29:41–99.
6. Dassonville O, Formento JL, Francoual M, Ramaioli A, Santini J, Schneider M, Demard F. Expression of epidermal growth factor receptor and survival in upper aerodigestive tract cancer. J Clin Oncol 1993;11:1873–8.
7. Sainsbury JR, Farndon JR, Needham GK, Malcolm AJ, Harris AL. Epidermal-growth-factor receptor status as predictor of early recurrence of and death from breast cancer. Lancet 1987;1:1398–402.
8. Scambia G, Benedetti-Panici P, Ferrandina G, Distefano M, Salerno G, Romanini ME, Fagotti A, Mancuso S. Epidermal growth factor, oestrogen and progesterone receptor expression in primary ovarian cancer: correlation with clinical outcome and response to chemotherapy. Br J Cancer 1995;72:361–6.
9. Veale D, Ashcroft T, Marsh C, Gibson GJ, Harris AL. Epidermal growth factor receptors in non-small cell lung cancer. Br J Cancer 1987;55:513–6.
10. Veale D, Kerr N, Gibson GJ, Kelly PJ, Harris AL. The relationship of quantitative epidermal growth factor receptor expression in non-small cell lung cancer to long term survival. Br J Cancer 1993;68:162–5.
11. Druker BJ, Talpaz M, Resta DJ, Peng B, Buchdunger E, Ford JM, Lydon NB, Kantarjian H, Capdeville R, Ohno-Jones S, Sawyers CL. Efficacy and safety of a specific inhibitor of the BCR-ABL tyrosine kinase in chronic myeloid leukemia. N Engl J Med 2001;344: 1031–7.
12. Druker BJ, Sawyers CL, Kantarjian H, Resta DJ, Reese SF, Ford JM, Capdeville R, Talpaz M. Activity of a specific inhibitor of the BCR-ABL tyrosine kinase in the blast crisis of chronic myeloid leukemia and acute lymphoblastic leukemia with the Philadelphia chromosome. N Engl J Med 2001;344:1038–42.
13. Joensuu H, Roberts PJ, Sarlomo-Rikala M, Andersson LC, Tervahartiala P, Tuveson D, Silberman S, Capdeville R, Dimitrijevic S, Druker B, Demetri GD. Effect of the tyrosine kinase inhibitor ST1571 in a patient with a metastatic gastrointestinal stromal tumor. N Engl J Med 2001;344:1052–6.
14. Fukuoka M, Yano S, Giaccone G, Tamura T, Nakagawa K, Douillard JY, Nishiwaki Y, Vansteenkiste J, Kudoh S, Rischin D, Eek R, Horai T, et al. Multi-institutional randomized phase II trial of gefitinib for previously treated patients with advanced non-small-cell lung cancer. J Clin Oncol 2003;21:2227–9.
15. Kris MG, Natale RB, Herbst RS, Lynch TJ Jr, Prager D, Belani CP, Schiller JH, Kelly K, Spiridonidis H, Sandler A, Albain KS, Cella D, et al. Efficacy of gefitinib, an inhibitor of the epidermal growth factor receptor tyrosine kinase, in symptomatic patients with non-small cell lung cancer: a randomized trial. JAMA 2003;290:2149–58.
16. Giaccone G, Johnson DH, Manegold C, et al. A phase III clinical trial of ZD1839 ('Iressa') in combination with gemcitabine and cisplatin in chemotherapy-naïve patients with advanced non-small-cell lung cancer (INTACT 1). Annual meeting of the European Society for Medical Oncology (ESMO). Nice, France, October 2002.
17. Miller VA, Johnson DH, Krug LM, Pizzo B, Tyson L, Perez W, Krozely P, Sandler A, Carbone D, Heelan RT, Kris MG, Smith R, et al. Pilot trial of the epidermal growth factor receptor tyrosine kinase inhibitor gefitinib plus carboplatin and paclitaxel in patients with stage IIIB or IV non-small-cell lung cancer. J Clin Oncol 2003;21: 2094–100.
18. Paez JG, Janne PA, Lee JC, Tracy S, Greulich H, Gabriel S, Herman P, Kaye FJ, Lindeman N, Boggon TJ, Naoki K, Sasaki H, et al. EGFR mutations in lung cancer: correlation with clinical response to gefitinib therapy. Science 2004;304:1497–500.
19. Lynch TJ, Bell DW, Sordella R, Gurubhagavatula S, Okimoto RA, Brannigan BW, Harris PL, Haserlat SM, Supko JG, Haluska FG, Louis DN, Christiani DC, et al. Activating mutations in the epidermal growth factor receptor underlying responsiveness of non-small-cell lung cancer to gefitinib. N Engl J Med 2004;350: 2191–3.
20. Pao W, Miller V, Zakowski M, Doherty J, Politi K, Sarkaria I, Singh B, Heelan R, Rusch V, Fulton L, Mardis E, Kupfer D, et al. EGF receptor gene mutations are common in lung cancers from "never smokers" and are associated with sensitivity of tumors to gefitinib and erlotinib. Proc Natl Acad Sci USA 2004; 101:13306–11.
21. Nomori H, Saijo N, Fujita J, Hyoi M, Sasaki Y, Shimizu E, Kanzawa F, Inomata M, Hoshi A. Detection of NK activity and antibody-dependent cellular cytotoxicity of lymphocytes by human tumor clonogenic assay—its correlation with the 51Cr-release assay. Int J Cancer 1985;35:449–55.
22. Mosmann T. Rapid colorimetric assay for cellular growth and survival: application to proliferation and cytotoxicity assays. J Immunol Meth 1983;65:55–63.
23. Arteaga CL, Ramsey TT, Shawver LK, Guyer CA. Unliganded epidermal growth factor receptor dimerization induced by direct interaction of quinazolines with ATP binding site. J Biol Chem 1998;273:18623–32.
24. Gorre ME, Mohammed M, Ellwood K, Hsu N, Paquette R, Rao PN, Sawyers CL. Clinical resistance to STI-571 cancer therapy caused by BCR-ABL gene mutation or amplification. Science 2001;293:876–80.
25. Von Bubnoff N. BCR-ABL gene mutation in relation to clinical resistance Lancet 2002;356:487–91.
26. McCormick F. New-age drug meets resistance. Nature 2001;412: 281–2.
27. Ricci C, Scappini B, Divoky V, Onida F, Verstovsek S, Kantarjian HM, Beran M. Mutation in the ATP binding pocket of the ABL kinase domain in and STI571-resistant BCR/ABL-positive cell line. Cancer Res 2002;62:5995–8.
28. Laffargue M, Raynal P, Yart A, Peres C, Wetzker R, Roche S, Payrastre B, Chap H. An epidermal growth factor receptor/Gab1 signaling pathway is required for activation of phosphoinositide 3-kinase by lysophosphatidic acid. J Biol Chem 1999;274:32835–41.
29. Rodriguez-Viciana P, Warne PH, Dhand R, Vanhaesebroeck B, Gout I, Fry MJ, Waterfield MD, Downward J. Phosphatidylinositol-3-OH kinase as a direct target of Ras. Nature 1994;370:527–32.
30. Kurata T, Tamura K, Kaneda H, Nogami T, Uejima H, Asai Go G, Nakagawa K, Fukuoka M. Effect of re-treatment with gefitinib ('Iressa', ZD1839) after acquisition of resistance. Ann Oncol 2004;15:173–4.
31. Sugimoto Y. Breast cancer resistance protein (BCRP): physiological substrates, reversing agents and SNPs. Abstract 21. 7th Int Symp Cancer Chemother 2002,Tokyo, Japan, 2002.
32. Naruse I, Ohmori T, Ao Y, Fukumoto H, Kuroki T, Mori M, Saijo N, Nishio K. Antitumor activity of the selective epidermal growth factor receptor- tyrosine kinase inhibitor (EGFR-TKI) Iressatm (ZD1839) in a EGFR-expressing multidrug resistant cell line in vitro and in vivo. Int J Cancer 2002;98:310–5.
33. Reynolds AR, Tischer C, Verveer PJ, Rocks O, Bastiaens PIH. EGFR activation coupled to inhibition of tyrosine phosphatases causes lateral signal propagation. Nat Cell Biol 2003;5:447–53.
34. Haj FG, Markova B, Klaman LD, Bohmer FD, Neel BG. Regulation of receptor tyrosine kinase signaling by protein tyrosine phosphatase-1B. J Biol Chem 2003;278:739–44.
35. Wu JY, Talpaz M, Donato NJ. Tyrosine kinases and phosphatase play a role in ST1571-mediate apoptosis of chronic myelogenous leukemia cells. Proc Am Assoc Cancer Res 2003;44.
36. Wakeling AE, Guy SP, Woodburn JR, Ashton SE, Curry BJ, Barker AJ, Gibson KH. ZD1839 (Iressa): an orally active inhibitor of epidermal growth factor signaling with potential for cancer therapy. Cancer Res 2002;62:5749–54.
37. Moasser MM, Basso A, Averbuch SD, Rosen N. The tyrosine kinase inhibitor ZD1839 ("Iressa") inhibits HER2-driven signaling and suppresses the growth of HER2-overexpressing tumor cells. Cancer Res 2001;61:7184–8.

VOLUME 23 · NUMBER 6 · FEBRUARY 20 2005

JOURNAL OF CLINICAL ONCOLOGY

ORIGINAL REPORT

Randomized Pharmacokinetic and Pharmacodynamic Study of Docetaxel: Dosing Based on Body-Surface Area Compared With Individualized Dosing Based on Cytochrome P450 Activity Estimated Using a Urinary Metabolite of Exogenous Cortisol

Noboru Yamamoto, Tomohide Tamura, Haruyasu Murakami, Tatsu Shimoyama, Hiroshi Nokihara, Yutaka Ueda, Ikuo Sekine, Hideo Kunitoh, Yuichiro Ohe, Tetsuro Kodama, Mikiko Shimizu, Kazuto Nishio, Naoki Ishizuka, and Nagahiro Saijo

From the Division of Internal Medicine, National Cancer Center Hospital, Pharmacology Division and Cancer Information and Epidemiology Division, National Cancer Center Research Institute, Tokyo, Japan

Submitted November 7, 2003; accepted August 19, 2004

Supported in part by a Grant-in-Aid for Cancer Research (0-25) from the Ministry of Health, Labor, and Welfare, Tokyo, Japan

Presented in part at the 38th Annual Meeting of the American Society of Clinical Oncology, May 18-21, 2002, Orlando, FL

Authors' disclosures of potential conflicts of interest are found at the end of this article

Address reprint requests to Tomohide Tamura, MD, Division of Internal Medicine, National Cancer Center Hospital, 5-1-1, Tsukiji, Chuo-ku, Tokyo, 104-0045, Japan; e-mail ttamura@ncc.go.jp

© 2005 by American Society of Clinical Oncology

0732-183X/05/2306-1061/$20.00

DOI: 10.1200/JCO.2005.11.036

ABSTRACT

Purpose

Docetaxel is metabolized by cytochrome P450 (CYP3A4) enzyme, and the area under the concentration-time curve (AUC) is correlated with neutropenia. We developed a novel method for estimating the interpatient variability of CYP3A4 activity by the urinary metabolite of exogenous cortisol (6-beta-hydroxycortisol [6-β-OHF]). This study was designed to assess whether the application of our method to individualized dosing could decrease pharmacokinetic (PK) and pharmacodynamic (PD) variability compared with body-surface area (BSA) –based dosing.

Patients and Methods

Fifty-nine patients with advanced non–small-cell lung cancer were randomly assigned to either the BSA-based arm or individualized arm. In the BSA-based arm, 60 mg/m^2 of docetaxel was administered. In the individualized arm, individualized doses of docetaxel were calculated from the estimated clearance (estimated clearance = 31.177 + [7.655 × 10^{-4} × total 6-β-OHF] − [4.02 × alpha-1 acid glycoprotein] − [0.172 × AST] − [0.125 × age]) and the target AUC of 2.66 mg/L · h.

Results

In the individualized arm, individualized doses of docetaxel ranged from 37.4 to 76.4 mg/m^2 (mean, 58.1 mg/m^2). The mean AUC and standard deviation (SD) were 2.71 (range, 2.02 to 3.40 mg/L · h) and 0.40 mg/L · h in the BSA-based arm, and 2.64 (range, 2.15 to 3.07 mg/L · h) and 0.22 mg/L · h in the individualized arm, respectively. The SD of the AUC was significantly smaller in the individualized arm than in the BSA-based arm ($P < .01$). The percentage decrease in absolute neutrophil count (ANC) averaged 87.1% (range, 59.0 to 97.7%; SD, 8.7) in the BSA-based arm, and 87.4% (range, 78.0 to 97.2%; SD, 6.1) in the individualized arm, suggesting that the interpatient variability in percent decrease in ANC was slightly smaller in the individualized arm.

Conclusion

The individualized dosing method based on the total amount of urinary 6-β-OHF after cortisol administration can decrease PK variability of docetaxel.

J Clin Oncol 23:1061-1069. © 2005 by American Society of Clinical Oncology

INTRODUCTION

Many cytotoxic drugs have narrow therapeutic windows despite having a large interpatient pharmacokinetic (PK) variability. The doses of these cytotoxic drugs are usually calculated on the basis of body-surface area (BSA). Although several physiologic functions are proportional to BSA, systemic exposure to a drug is only partially related to

Downloaded from www.jco.org at National Cancer Center on May 6, 2005 .
Copyright © 2005 by the American Society of Clinical Oncology. All rights reserved.

this parameter.[1-3] Consequently, a large interpatient PK variability is seen when doses are based on BSA. This large interpatient PK variability can result in undertreatment with inappropriate therapeutic effects in some patients, or in overtreatment with unacceptable severe toxicities in others. Understanding interpatient PK variability is important for optimizing anticancer treatments. Factors that affect PK variability include drug absorption, metabolism, and excretion. Among these factors, drug metabolism is regarded as a major factor causing PK variability. Unfortunately, however, no simple and practical method for estimating the interpatient variability of drug metabolism is available. If drug metabolism in each patient could be predicted, individualized dosing could be performed to optimize drug exposure while minimizing unacceptable toxicity.

Docetaxel is a cytotoxic agent that promotes microtubule assembly and inhibits depolymerization to free tubulin, resulting in the blockage of the M phase of the cell cycle.[4] Docetaxel has shown promising activity against several malignancies, including non–small-cell lung cancer, and is metabolized by hepatic CYP3A4 enzyme.[5-15]

Human CYP3A4 is a major cytochrome P450 enzyme that is present abundantly in human liver microsomes and is involved in the metabolism of a large number of drugs, including anticancer drugs.[16-18] This enzyme exhibits a remarkable interpatient variation in activity as high as 20-fold, which accounts for the large interpatient differences in the disposition of drugs that are metabolized by this enzyme.[19-22] Several noninvasive in vivo probes for estimating the interpatient variability of CYP3A4 activity have been reported and include the erythromycin breath test, the urinary dapsone recovery test, measurement of midazolam clearance (CL), and measurement of the ratio of endogenous urinary 6-beta-hydroxycortisol (6-β-OHF) to free-cortisol (FC).[23-27] The erythromycin breath test and the measurement of midazolam CL are the best validated, and both have been shown to predict docetaxel CL in patients.[28,29] However, neither probe has been used in a prospective study to validate the correlations observed, or to test their utility in guiding individualized dosing.

We developed a novel method for estimating the interpatient variability of CYP3A4 activity by urinary metabolite of exogenous cortisol. The total amount of 24-hour urinary 6-β-OHF after cortisol administration (total 6-β-OHF) is significantly correlated with docetaxel CL, which is metabolized by the CYP3A4 enzyme. We also illustrate the possibility that individualized dosing to optimize drug exposure and decrease interpatient PK variability could be performed using this method.[30]

We conducted a prospective, randomized PK and pharmacodynamic (PD) study of docetaxel comparing BSA-based dosing and individualized dosing based on the interpatient variability of CYP3A4 activity, as estimated by a urinary metabolite of exogenous cortisol. The objective of this study was to assess whether the application of our method to individualized dosing could decrease PK and PD variability of docetaxel compared with BSA-based dosing.

PATIENTS AND METHODS

Patient Selection

Patients with histologically or cytologically documented advanced or metastatic non-small-cell lung cancer were eligible for this study. Other eligibility criteria included the following: age $\geq$ 20 years; Eastern Cooperative Oncology Group performance status of 0, 1, or 2; 4 weeks of rest since any previous anticancer therapy; and adequate bone marrow (absolute neutrophil count [ANC] $\geq$ 2,000/μL and platelet count $\geq$ 100,000/μL), renal (serum creatinine level $\leq$ 1.5 mg/dL), and hepatic (serum total bilirubin level $\leq$ 1.5 mg/dL, AST level $\leq$ 150 U/L, and ALT level $\leq$ 150 U/L) function. Written informed consent was obtained from all patients before enrollment onto the study.

The exclusion criteria included the following: pregnancy or lactation; concomitant radiotherapy for primary or metastatic sites; concomitant chemotherapy with any other anticancer agents; treatment with steroids or any other drugs known to induce or inhibit CYP3A4 enzyme[17]; serious pre-existing medical conditions, such as uncontrolled infections, severe heart disease, diabetes, or pleural or pericardial effusions requiring drainage; and a known history of hypersensitivity to polysorbate 80. This study was approved by the institutional review board of the National Cancer Center.

Pretreatment and Follow-Up Evaluation

On enrollment onto the study, a history and physical examination were performed, and a complete differential blood cell count (including WBC count, ANC, hemoglobin, and platelets), and a clinical chemistry analysis (including serum total protein, albumin [ALB], bilirubin, creatinine, AST, ALT, gamma-glutamyltransferase, alkaline phosphatase [ALP], and alpha-1 acid glycoprotein [AAG]) were performed. Blood cell counts and a chemistry analysis except for AAG were performed at least twice a week throughout the study. Tumor measurements were performed every two cycles, and antitumor response was assessed by WHO standard response criteria. Toxicity was evaluated according to the National Cancer Institute Common Toxicity Criteria (version 2.0).

Study Design

This study was designed to assess whether the application of our method to individualized dosing could decrease PK and PD variability compared with BSA-based dosing. The primary end point was PK variability and the secondary end point was PD variability (ie, toxicity). In our previous study involving 29 patients who received 60 mg/m^2 of docetaxel, the area under the concentration-time curve (AUC) was calculated to be 2.66 $\pm$ 0.91 (mean $\pm$ standard deviation [SD]) mg/L $\cdot$ h.[30] We assumed that the variability of AUC, represented by the SD, could be reduced by 50% in the individualized arm compared with that in the BSA-based arm, and that AUC would be normally distributed. The required sample size was 25 patients per arm to detect this difference with a two-sided F test at α = .05 and a power of 0.914.

Patients were randomly assigned to either the BSA-based arm or individualized arm (Fig 1). In the BSA-based arm, each patient received a dose of 60 mg/m^2 of docetaxel. In the individualized arm, individualized doses of docetaxel were calculated from the estimated docetaxel CL after cortisol administration and the target AUC (described in the Docetaxel Administration section).

Cortisol Administration and Urine Collection

In the individualized arm, 300 mg of hydrocortisone (Banyu Pharmaceuticals Co, Tokyo, Japan) was diluted in 100 mL of 0.9%

Downloaded from www.jco.org at National Cancer Center on May 6, 2005 .
Copyright © 2005 by the American Society of Clinical Oncology. All rights reserved.

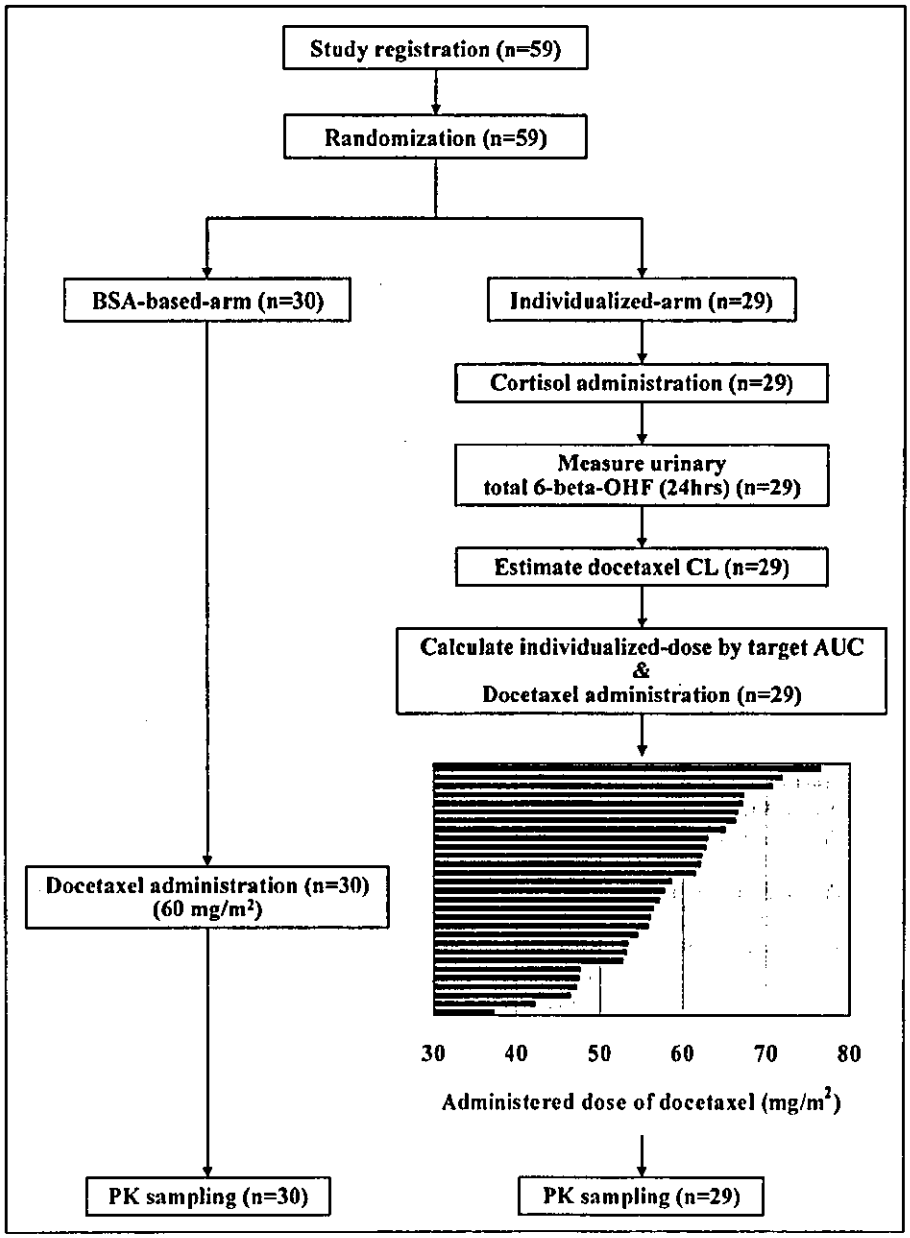

Fig 1. Study flow diagram and administered dose of docetaxel. PK, pharmacokinetic; AUC, area under the concentration-time curve; CL, clearance; 6-β-OHF, 6-beta-hydroxycortisol

saline and administered intravenously for 30 minutes at 9 AM on day 1 in all patients to estimate the interpatient variability of CYP3A4 activity. After cortisol administration, the urine was collected for 24 hours. The total volume of the 24-hour collection was recorded, and a 5-mL aliquot was analyzed immediately.

Docetaxel Administration

Docetaxel (Taxotere; Aventis Pharm Ltd, Tokyo, Japan) was obtained commercially as a concentrated sterile solution containing 80 mg of the drug in 2 mL of polysorbate 80. In the BSA-based arm, a dose of 60 mg/m² of docetaxel was diluted in 250 mL of 5% glucose or 0.9% saline and administered by 1-hour intravenous infusion at 9 AM to all patients.

In the individualized arm, individualized dose of docetaxel was calculated from the estimated CL and the target AUC of 2.66 mg/L · h using the following equations:

$$\text{Estimated CL (L/h/m}^2) = 31.177 + (7.655 \times 10^{-4} \times \text{total-6-}\beta\text{-OHF [}\mu\text{g/dl]}) - (4.02 \times \text{AAG [g/L]}) - (0.172 \times \text{AST [U/L]}) - (0.125 \times \text{age [years]})^{[6]}$$

$$\text{Individualized dose of docetaxel (mg/m}^2) = \text{estimated docetaxel CL (L/h/m}^2) \times \text{target AUC (2.66 mg/L} \cdot \text{h)}$$

Downloaded from www.jco.org at National Cancer Center on May 6, 2005 .
Copyright © 2005 by the American Society of Clinical Oncology. All rights reserved.

At least 2 days after cortisol administration, individualized doses of docetaxel were diluted in 250 mL of 5% glucose or 0.9% saline and administered by 1-hour intravenous infusion at 9 AM to each patient. The doses of docetaxel in subsequent cycles of treatment were unchanged, and no prophylactic premedication to protect against docetaxel-related hypersensitivity reactions was administered in either of the treatment arms.

PK Study

Blood samples for PK studies were obtained from all of the patients during the initial treatment cycle. An indwelling cannula was inserted in the arm opposite that used for the drug infusion, and blood samples were collected into heparinized tubes. Blood samples were collected before the infusion; 30 minutes after the start of the infusion; at the end of the infusion; and 15, 30, and 60 minutes and 3, 5, 9, and 24 hours after the end of the infusion. All blood samples were centrifuged immediately at 4,000 rpm for 10 minutes, after which the plasma was removed and the samples were placed in polypropylene tubes, labeled, and stored at −20°C or colder until analysis.

PK parameters were estimated by the nonlinear least squares regression analysis method (WinNonlin, Version 1.5; Bellkey Science Inc, Chiba, Japan) with a weighting factor of 1 per year.[2] Individual plasma concentration-time data were fitted to two- and three-compartment PK models using a zero-order infusion input and first-order elimination. The model was chosen on the basis of Akaike's information criteria.[31] The peak plasma concentration (C_{max}) was generated directly from the experimental data. AUC was extrapolated to infinity and determined based on the best-fitted curve; this measurement was then used to calculate the absolute CL (L/h), defined as the ratio of the delivered dosage (in milligrams) and AUC.

To assess PD effect of docetaxel, the percentage decrease in ANC was calculated according to the following formula: % decrease in ANC = (pretreatment ANC − nadir ANC)/(pretreatment ANC) × 100.

Measurements

The concentration of urinary 6-β-OHF was measured by reversed phase high-performance liquid chromatography with UV absorbance detection according to previously published methods.[30,32,33]

Docetaxel concentrations in plasma were also measured by solid-phase extraction and reversed phase high-performance liquid chromatography with UV detection according to the previously published method.[30,34] The detection limit corresponded to a concentration of 10 ng/mL.

Statistical Analysis

Fisher's exact test or χ^2 test was used to compare categoric data, and Student's t test was used for continuous variables. The strength of the relationship between the estimated docetaxel CL and the observed docetaxel CL was assessed by least squares linear regression analysis. The interpatient variability of AUC for each arm was evaluated by determining the SD and was compared by F test. Biases, or the mean AUC value in each arm minus the target AUC (2.66 mg/L · h), were also compared between the arms by Student's t test.

A two-sided P value of ≤ .05 or less was considered to indicate statistical significance. All statistical analyses were performed using SAS software version 8.02 (SAS Institute, Cary, NC).

RESULTS

Patient Characteristics

Between October 1999 and May 2001, 59 patients were enrolled onto the study and randomly assigned to either the BSA-based arm (n = 30) or the individualized arm (n = 29). All 59 patients were assessable for PK and PD analyses. The pretreatment characteristics of the 59 patients are listed in Table 1. The baseline characteristics were well balanced between the arms except for three laboratory parameters: ALB, AAG, and ALP. These three parameters were not included in the eligibility criteria. The majority of patients (95%) had a performance status of 0 or 1. Twenty (67%) and 16 (55%) patients had been treated with platinum-based chemotherapy in the BSA-based arm and individualized arm, respectively. Only two patients in the individualized arm had liver metastasis, and most of the patients had good hepatic functions.

Individualized Dosing of Docetaxel

In the individualized arm, the total amount of 24-hour urinary 6-β-OHF after cortisol administration (total 6-β-OHF) was 9,179.6 ± 3,057.7 μg/d (mean ± SD), which was similar to the result of our previous study.[30] The estimated docetaxel CL was 21.9 ± 3.5 L/h/m^2 (mean ± SD), and individualized dose of docetaxel ranged from 37.4 to 76.4 mg/m^2 (mean, 58.1 mg/m^2; Fig 1).

PK

Docetaxel PK data were obtained from all 59 patients during the first cycle of therapy, and PK parameters are listed in Table 2. Drug levels declined rapidly after infusion and could be determined to a maximum of 25 hours. The concentration of docetaxel in plasma was fitted to a biexponential equation, which was consistent with previous reports.[30,35-38] The mean alpha and beta half-lives were 9.2 minutes and 5.0 hours in the BSA-based arm and 9.2 minutes and 7.4 hours in the individualized arm, respectively.

In the BSA-based arm, docetaxel CL was 22.6 ± 3.4 L/h/m^2 (mean ± SD), and AUC averaged 2.71 mg/L · h (range, 2.02 to 3.40 mg/L · h). In the individualized arm, docetaxel CL was 22.1 ± 3.4 L/h/m^2, and AUC averaged 2.64 mg/L · h (range, 2.15 to 3.07 mg/L · h). The least squares linear regression analysis showed that the observed docetaxel CL was well estimated in the individualized arm (r^2 = 0.821; Fig 2).

The SDs of AUC in the BSA-based arm and in the individualized arm were 0.40 and 0.22, respectively, and the ratio of SD in the individualized arm to that in the BSA-based arm was 0.538 (95% CI, 0.369 to 0.782). The biases from the target AUC in the BSA-based arm and in the individualized arm were 0.047 (95% CI, −0.104 to 0.198) and −0.019 (95% CI, −0.102 to 0.064), respectively, with no significant difference. The interpatient variability of

Downloaded from www.jco.org at National Cancer Center on May 6, 2005 .
Copyright © 2005 by the American Society of Clinical Oncology. All rights reserved.

Table 1. Patient Characteristics

Characteristic	BSA Based Arm No. of Patients	%	Individualized Arm No. of Patients	%	P
Enrolled	30		29		
Eligible	30	100	29	100	
Age, years					.62
Median	61		62		
Range	52-73		45-73		
Sex					
Male	25	83	19	66	14
Female	5	17	10	34	
ECOG PS					
0	7	23	1	3	.08
1	22	73	26	90	
2	1	3	2	7	
Prior treatment					
None	4	13	4	14	.99
Surgery	11	37	9	31	.65
Radiotherapy	13	43	10	34	.49
Chemotherapy	21	70	18	62	.52
Platinum-based regimens	20	67	16	55	.37
Site of disease					
Lung	23	77	28	97	.10
Liver	0	0	2	7	.24
Pleura	8	27	12	41	.23
Bone	7	23	9	31	.71
Extrathoracic lymph nodes	0	33	10	34	.93
Laboratory parameters					
ALB, g/L					.02
Median	38		35		
Range	26-45		24-44		
AAG, g/L					.04
Median	1.00		1.25		
Range	0.28-2.15		0.64-2.54		
AST, U/L					.67
Median	21		22		
Range	10-40		7-41		
ALT, U/L					.88
Median	18		18		
Range	6-54		4-45		
ALP, U/L					.03
Median	249		324		
Range	129-540		185-986		

Abbreviations: ECOG, Eastern Cooperative Oncology Group; PS, performance status; ALB, serum albumin; AAG, alpha-1-acid glycoprotein; ALP, serum alkaline phosphatase.

AUC was significantly smaller in the individualized arm than in the BSA-based arm ($P < .01$; Fig 3).

PD

In both arms, neutropenia was the predominant toxicity related to docetaxel treatment, and 28 of 30 (93%) patients in the BSA-based arm and 25 of 29 (86%) patients in the individualized arm had grade 3 or 4 neutropenia.

Table 2. Docetaxel PK Parameters

Parameters	BSA-Based Arm (n = 30)	Individualized Arm (n = 29)
C_{max}, μg/mL	0.36-2.70	0.99-2.41
$t_{1/2}$ alpha*, minutes	9.2 ± 3.3	9.2 ± 2.7
$t_{1/2}$ beta*, hours	5.0 ± 4.8	7.4 ± 11.7
CL* L/h	37.6 ± 6.3	34.8 ± 7.1
CL* L/h/m²	22.6 ± 3.4	22.1 ± 3.4
AUC		
Mean mg/L · h	2.71	2.64
Range mg/L · h	2.02-3.40	2.15-3.07
Median	2.65	2.66
SD	0.40	0.22

Abbreviations: PK, pharmacokinetic; BSA, body-surface area; CL, clearance; AUC, area under concentration-time curve; SD, standard deviation.
*Data represent mean ± SD.

Nonhematologic toxicities, such as gastrointestinal and hepatic toxicities (ie, hyperbilirubinemia, aminotransferase elevations), were mild in both arms.

PD effects shown as the percentage decrease in ANC are listed in Table 3. The percentage decrease in ANC for the BSA-based arm and individualized arm were 87.1% (range, 59.0 to 97.7%; SD, 8.7) and 87.5% (range, 78.0 to 97.2%; SD, 6.1), respectively, suggesting that the interpatient variability in the percentage decrease in ANC was slightly smaller in the individualized arm than in the BSA-based arm (Fig 4). The response rates between the two arms were similar; five of 30 (16.7%) and four of 29 (13.8%) patients

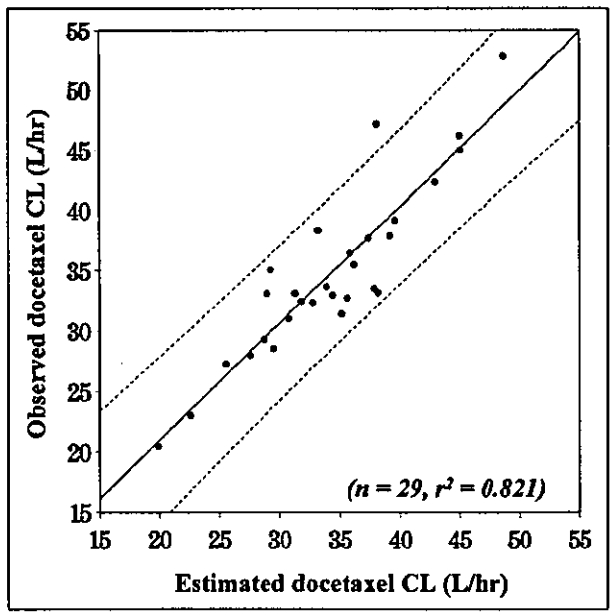

Fig 2. Correlation between the estimated and observed docetaxel clearance (CL) in the individualized arm (n = 29). (—) Linear regression line (r^2 = 0.821). (- - -) 95% CIs for individual estimates.

Downloaded from www.jco.org at National Cancer Center on May 6, 2005 .
Copyright © 2005 by the American Society of Clinical Oncology. All rights reserved.

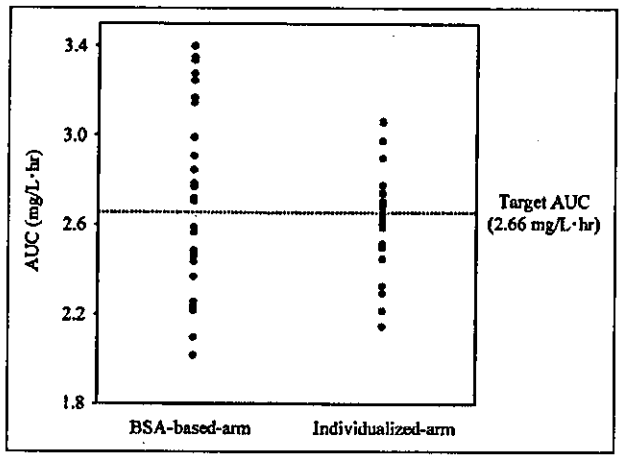

Fig 3. Comparison of area under the concentration-time curve (AUC) variability between the arms ($P < .01$; F test) BSA, body-surface area.

achieved a partial response in the BSA-based arm and individualized arm, respectively.

DISCUSSION

In oncology practice, the prescribed dose of most anticancer drugs is currently calculated from BSA of individual patients to reduce the interpatient variability of drug exposure. However, PK parameters, such as CL of many anticancer drugs, are not related to BSA.[2,39,43] Although PK parameters of docetaxel are correlated with BSA, individualized dosing based on individual metabolic capacities could further decrease the interpatient variability.[43]

CYP3A4 plays an important role in the metabolism of many drugs, including anticancer agents such as docetaxel, paclitaxel, vinorelbine, and gefitinib. This enzyme exhibits a large interpatient variability in metabolic activity, accounting for the large interpatient PK and PD variability. We have developed a novel method of estimating the interpatient variability of CYP3A4 activity by urinary metabolite of exogenous cortisol. That is, the total amount of 24-hour urinary 6-β-OHF after cortisol administration was highly correlated with docetaxel CL. We conducted a prospective randomized PK and PD study of docetaxel to evaluate whether the application of our method to individualized dosing could decrease PK and PD variability compared with BSA-based dosing.

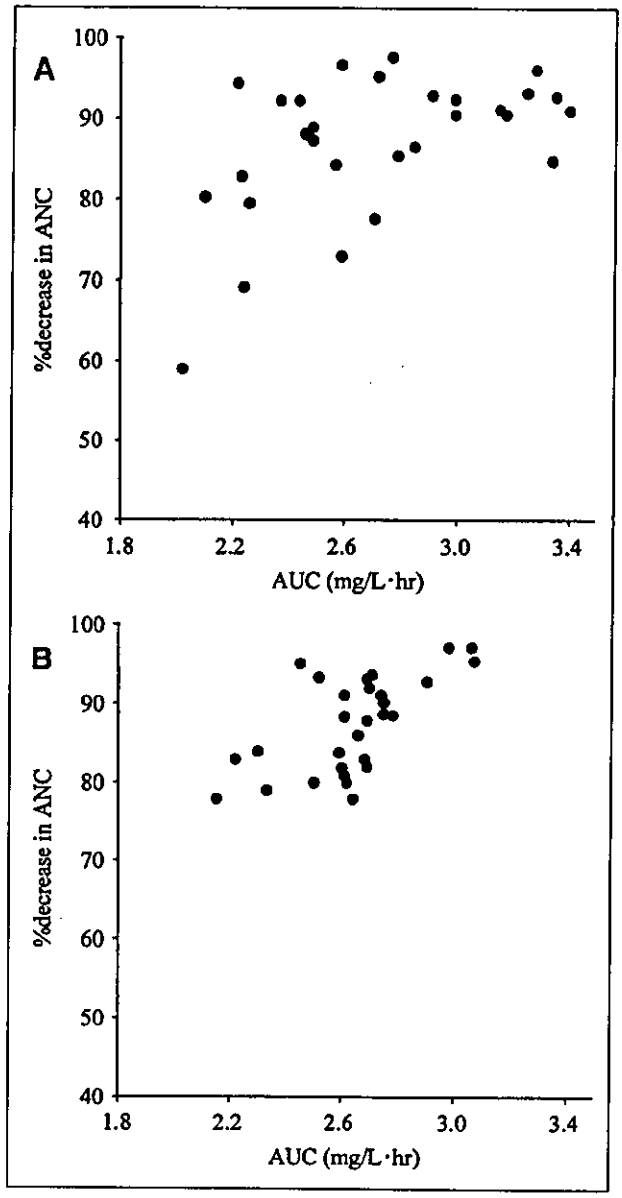

Fig 4. Correlation between area under the concentration-time curve (AUC) and percentage decrease in absolute neutrophil count (ANC) in each arm. (A) body-surface area–based arm; (B) individualized arm.

Table 3. Percentage Decrease in ANC

Parameters	BSA-Based Arm (n = 30)	Individualized Arm (n = 29)
Percentage decrease in ANC, %		
Mean	87.1	87.4
Range	59.0-97.7	78.0-97.2
Median	89.7	88.4
SD	8.7	8.1

Abbreviations: ANC, absolute neutrophil count; BSA, body-surface area; SD, standard deviation.

The study by Hirth et al[28] showed a good correlation between the result of the erythromycin breath test and docetaxel CL, and the study by Goh et al[29] showed a good correlation between the midazolam CL and docetaxel CL. In our study, we prospectively validated the correlation between docetaxel CL and our previously published method using the total amount of urinary 6-β-OHF after

Downloaded from www.jco.org at National Cancer Center on May 6, 2005 .
Copyright © 2005 by the American Society of Clinical Oncology. All rights reserved.

cortisol administration in the individualized arm. As shown in Fig 2, the observed docetaxel CL was well estimated, and the equation for the estimation of docetaxel CL developed in our previous study was found to be reliable and reproducible. The target AUC in the individualized arm was set at 2.66 mg/L · h. This value was the mean value from our previous study, in which 29 patients were treated with 60 mg/m^2 of docetaxel. Individualized doses of docetaxel ranged from 37.4 to 76.4 mg/m^2 and were lower than expected.

The SD of AUC in the individualized arm was about 46.2% smaller than that in the BSA-based arm, a significant difference; this result seems to indicate that the application of our method to individualized dosing can reduce the interpatient PK variability. Assuming that the variability of AUC could be decreased 46.2% by individualized dosing applying our method, overtreatment could be avoided in 14.5% of BSA-dosed patients by using individualized dosing (Fig 5, area A), and undertreatment could be avoided in another 14.5% of these patients (Fig 5, area B). We considered that neutropenia could be decreased with patients in area A by individualized dosing. However, it is unknown whether the therapeutic effect of docetaxel could be improved in the patients in area B by individualized dosing because no significant positive correlation has been found between docetaxel AUC and antitumor response in patients with non–small-cell lung cancer.[43] In this study, seven of 30 (23.3%) and two of 30 (6.7%) patients in the BSA-based arm were included in area A and B, respectively (Figs 3 and 5).

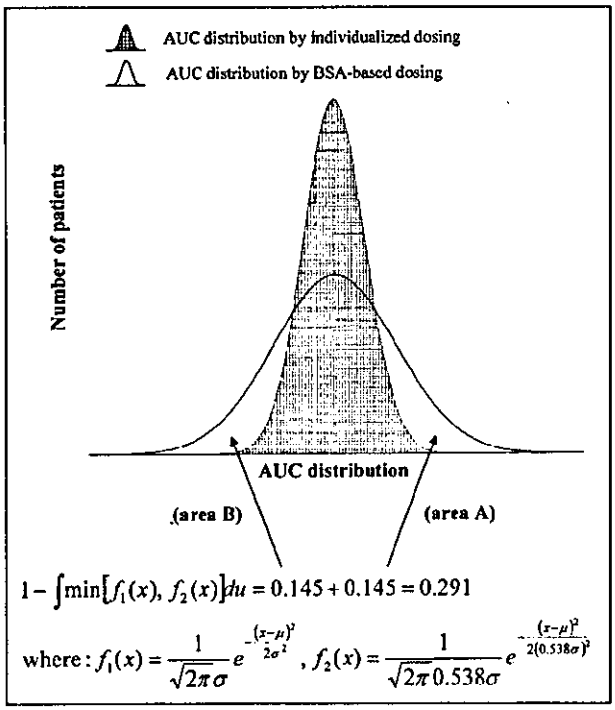

Fig 5. Simulated comparison of area under the concentration-time curve (AUC) distribution between body-surface area (BSA) - based dosing and individualized dosing when the variability of AUC is decreased 46.2% by individualized dosing applied using our method

As shown in Figure 4, the percentage decrease in ANC was well correlated with AUC in both arms, which was similar to previous reports.[37,43] It was also indicated that the interpatient variability in the percentage decrease in ANC was slightly smaller in the individualized arm than in the BSA-based arm; however, this difference was not significant. The response rates between the two arms were similar. Although the interpatient PK variability could be decreased by individualized dosing in accordance with our method, the interpatient PD variability such as toxicity and the antitumor response could not be decreased. Several reasons could be considered.

With regard to toxicity, the pretreatment characteristics of the patients in this study were highly variable. More than half of the patients in each arm had previously received platinum-based chemotherapy, and more than 30% had received radiotherapy. The laboratory parameters (ie, ALB, AAG, and ALP) were not balanced across the arms, although they were not included in the eligibility criteria (Table 1). These variable pretreatment characteristics and unbalanced laboratory parameters may have influenced the frequency and severity of the hematologic toxicity as well as the pharmacokinetic profiles. The antitumor effect may have been influenced by the intrinsic sensitivity of tumors, the variable pretreatment characteristics, and the imbalance in laboratory parameters. Non–small-cell lung cancer is a chemotherapy-resistant tumor. The response rate for docetaxel ranges from 18% to 38%,[5] and no significant positive correlation between docetaxel AUC and antitumor response has been found. We considered it quite difficult to control the interpatient PD variability by controlling the interpatient PK variability alone. Although we did not observe any outliers in either arm, such as the two outliers with severe toxicity observed in the study by Hirth et al,[28] our method may be more useful for identifying such outliers. If we had not excluded patients with more abnormal liver function or a history of liver disease by the strict eligibility criteria, the results with the two dosing regimens may have been more different, and the interpatient PD variability, such as the percentage decrease in ANC, may have been smaller in the individualized arm than in the BSA-based arm. Furthermore, the primary end point of this study was PK variability, evaluated by the SD of AUC in both arms, and the sample size was significantly underpowered to evaluate whether the application of our method to individualized dosing could decrease PD variability compared with BSA-based dosing.

For the genotypes of CYP3A4, several genetic polymorphisms have been reported (http://www.imm.ki.se/CYPalleles/); however, a clear relationship between genetic polymorphisms and the enzyme activity of CYP3A4 has not been reported. Our phenotype-based

Downloaded from www.jco.org at National Cancer Center on May 6, 2005 .
Copyright © 2005 by the American Society of Clinical Oncology. All rights reserved.

individualized dosing using the total amount of urinary 6-β-OHF after cortisol administration produced good results. However, this method is somewhat complicated, and a simpler method would be of great use. We analyzed the expression of CYP3A4 mRNA in the peripheral-blood mononuclear cells of the 29 patients in the individualized arm. No correlation was observed between the expression level of CYP3A4 mRNA and docetaxel CL or the total amount of urinary 6-β-OHF after cortisol administration (data not shown).

In conclusion, the individualized dosing of docetaxel using the total amount of urinary 6-β-OHF after cortisol administration is useful for decreasing the interpatient PK variability compared with the conventional BSA-based method of dosing. This method may be useful for individualized chemotherapy.

Authors' Disclosures of Potential Conflicts of Interest

The authors indicated no potential conflicts of interest.

REFERENCES

1. Sawyer M, Ratain MJ: Body surface area as a determinant of pharmacokinetics and drug dosing. Invest New Drugs 19:171-177, 2001
2. Gurney H: Dose calculation of anticancer drugs: A review of the current practice and introduction of an alternative. J Clin Oncol 14: 2590-2611, 1996
3. Ratain MJ: Body-surface area as a basis for dosing of anticancer agents: Science, myth, or habit? J Clin Oncol 16:2297-2298, 1998
4. Ringel I, Horwitz SB: Studies with RP 56976 (Taxotere): A semisynthetic analogue of taxol. J Natl Cancer Inst 83:288-291, 1991
5. Cortes JE, Pazdur R: Docetaxel. J Clin Oncol 13:2643-2655, 1995
6. Fossella FV, Lee JS, Murphy WK, et al: Phase II study of docetaxel for recurrent or metastatic non-small-cell lung cancer. J Clin Oncol 12:1238-1244, 1994
7. Fossella FV, Lee JS, Shin DM, et al: Phase II study of docetaxel for advanced or metastatic platinum refractory non-small cell lung cancer. J Clin Oncol 13:645-651, 1995
8. Gandara DR, Vokes E, Green M, et al: Activity of docetaxel in platinum-treated non-small cell lung cancer: Results of a phase II multicenter trial. J Clin Oncol 18:131-135, 2000
9. Kunitoh H, Watanabe K, Onoshi T, et al: Phase II trial of docetaxel in previously untreated advanced non-small-cell lung cancer: A Japanese cooperative study. J Clin Oncol 14:1649-1655, 1996
10. Fossella FV, DeVore R, Kerr RH, et al: Randomized phase III trial of docetaxel versus vinorelbine or ifosfamide in patients with advanced non-small cell lung cancer previously treated with platinum-containing chemotherapy regimens. The TAX 320 Non-Small Cell Lung Cancer Study Group. J Clin Oncol 18:2354-2362, 2000
11. Shepherd FA, Dancey J, Ramlau R, et al: Prospective randomized trial of docetaxel versus best supportive care in patients with non-small-cell lung cancer previously treated with platinum-based chemotherapy. J Clin Oncol 18:2095-2103, 2000
12. Hudis CA, Seidman AD, Crown JP, et al: Phase II and pharmacologic study of docetaxel as initial chemotherapy for metastatic breast cancer. J Clin Oncol 14:58-65, 1996
13. Trudeau ME, Eisenhauer EA, Higgins BP, et al: Docetaxel in patients with metastatic breast cancer: A phase II study of the National Cancer Institute of Canada-Clinical Trials Group. J Clin Oncol 14:422-428, 1996
14. Chan S, Friedrichs K, Noel D, et al: Prospective randomized trial of docetaxel versus doxorubicin in patients with metastatic breast cancer: The 303 Study Group. J Clin Oncol 17:2341-2354, 1999
15. Marre F, Sanderink GJ, de Sousa G, et al: Hepatic biotransformation of docetaxel (Taxotere) *in vitro*: Involvement of the CYP3A subfamily in humans. Cancer Res 56:1296-1302, 1996
16. Nelson DR, Koymans L, Kamataki T, et al: P450 superfamily: Update on new sequences, gene mapping, accession numbers and nomenclature. Pharmacogenetics 6:1-42, 1996
17. Lin JH, Lu AYH: Inhibition and induction of cytochrome P450 and the clinical implications. Clin Pharmacokinet 35:361-390, 1998
18. Parkinson A: An overview of current cytochrome P450 technology for assessing the safety and efficacy of new materials. Toxicol Pathol 24:45-57, 1996
19. Shimada T, Yamazaki H, Mimura M, et al: Interindividual variations in human liver cytochrome P-450 enzymes involved in the oxidation of drugs, carcinogens and toxic chemicals: Studies with liver microsomes of 30 Japanese and 30 Caucasians. J Pharmacol Exp Ther 270:414-423, 1994
20. Guengerich FP: Characterization of human microsomal cytochrome P450 enzymes. Annu Rev Pharmacol Toxicol 29:241-264, 1989
21. Guengerich FP, Turvy CG: Comparison of levels of human microsomal cytochrome P450 enzymes and epoxide hydrolase in normal and disease status using immunochemical analysis of surgical samples. J Pharmacol Exp Ther 256: 1189-1194, 1991
22. Hunt CM, Westerkam WR, Stave GM: Effects of age and gender on the activity of human hepatic CYP3A. Biochem Pharmacol 44: 275-283, 1992
23. Watkins PB, Turgeon DK, Saenger P, et al: Comparison of urinary 6-beta-cortisol and the erythromycin breath test as measures of hepatic P450IIIA (CYP3A) activity. Clin Pharmacol Ther 52:265-273, 1992
24. Kinirons MT, O'Shea D, Downing TF, et al: Absence of correlations among three putative *in vivo* probes of human cytochrome P4503A activity in young healthy men. Clin Pharmacol Ther 54:621-629, 1993
25. Hunt CM, Watkins PB, Saenger P, et al: Heterogeneity of CYP3A isoforms metabolizing erythromycin and cortisol. Clin Pharmacol Ther 51:18-23, 1992
26. Thummel KE, Shen DD, Podoll TD, et al: Use of midazolam as a human cytochrome P450 3A probe: II. Characterization of inter- and intra-individual hepatic CYP3A variability after liver transplantation. J Pharmacol Exp Ther 271:557-566, 1994
27. Thummel KE, Shen DD, Podoll TD, et al: Use of midazolam as a human cytochrome P450 3A probe: I. In vitro-in vivo correlations in liver transplant patients. J Pharmacol Exp Ther 271: 549-556, 1994
28. Hirth J, Watkins PB, Strawderman M, et al: The effect of an individual's cytochrome CYP3A4 activity on docetaxel clearance. Clin Cancer Res 6:1255-1258, 2000
29. Goh BC, Lee SC, Wang LZ, et al: Explaining interindividual variability of docetaxel pharmacokinetics and pharmacodynamics in Asians through phenotyping and genotyping strategies. J Clin Oncol 20:3683-3690, 2002
30. Yamamoto N, Tamura T, Kamiya Y, et al: Correlation between docetaxel clearance and estimated cytochrome P450 activity by urinary metabolite of exogenous cortisol. J Clin Oncol 18:2301-2308, 2000
31. Yamaoka K, Nakagawa T, Uno T: Application of Akaike's information criterion (AIC) in the evaluation of linear pharmacokinetic equations. J Pharmacokinet Biopharm 6:165-175, 1978
32. Nakamura J, Yakata M: Determination of urinary cortisol and 6 beta-hydroxycortisol by high performance liquid chromatography. Clin Chim Acta 149:215-224, 1985
33. Lykkesfeldt J, Loft S, Poulsen HE: Simultaneous determination of urinary free cortisol and 6 beta hydroxycortisol by high performance liquid chromatography to measure human CYP3A activity. J Chromatogr B Biomed Appl 660:23-29, 1994
34. Vergniol JC, Bruno R, Montay G, et al: Determination of Taxotere in human plasma by a semi-automated high-performance liquid chromatographic method. J Chromatogr 582:273-278, 1992
35. Taguchi T, Furue H, Nitani H, et al: Phase I clinical trial of RP 56976 (docetaxel): a new anticancer drug. Gan To Kagaku Ryoho 21:1997-2005, 1994
36. Burris H, Irvin B, Kuhn J, et al: Phase I clinical trial of Taxotere administered as either a 2 hour or 6 hour intravenous infusion. J Clin Oncol 11:950-958, 1993
37. Extra JM, Rousseau F, Bruno R, et al: Phase I and pharmacokinetic study of Taxotere (RP 56976; NSC 628503) given as a short

Downloaded from www.jco.org at National Cancer Center on May 6, 2005.
Copyright © 2005 by the American Society of Clinical Oncology. All rights reserved.

intravenous infusion. Cancer Res 53:1037-1042, 1993

38. Pazdur R, Newman RA, Newman BM, et al: Phase I trial of Taxotere: Five-day schedule. J Natl Cancer Inst 84:1781-1788, 1992

39. Mathijssen RHJ, Verweij J, de Jonge MJ, et al: Impact of body-size measures on irinotecan clearance: Alternative dosing recommendations. J Clin Oncol 20:81-87, 2002

40. De Jongh FE, Verweij J, Loos WJ, et al: Body-surface area-based dosing does not increase accuracy of predicting cisplatin exposure. J Clin Oncol 19:3733-3739, 2001

41. Gurney HP, Ackland S, Gebski V, et al: Factors affecting epirubicin pharmacokinetics and toxicity: Evidence against using body-surface area for dose calculation. J Clin Oncol 16:2299-2304, 1998

42. Loos WJ, Gelderblom H, Sparreboom A, et al: Inter- and intrapatient variability in oral topotecan pharmacokinetics: Implications for body-surface area dosage regimens. Clin Cancer Res 6:2685-2689, 2000

43. Bruno R, Hille D, Riva A, et al: Population pharmacokinetics/pharmacodynamics of docetaxel in phase II studies in patients with cancer. J Clin Oncol 16:187-196, 1998

Attention Authors: You Asked For It - You Got It!

Online Manuscript System Launched November 1st

On November 1st, *JCO* formally introduced its online Manuscript Processing System that will improve all aspects of the submission and peer-review process. Authors should notice a quicker turnaround time from submission to decision through this new system.

Based on the well known Bench>Press system by HighWire Press, the *JCO* Manuscript Processing System promises to further *JCO*'s reputation of providing excellent author service, which includes an already fast turnaround time of 7 weeks from submission to decision, no submission fees, no page charges, and allowing authors to freely use their work that has appeared in the journal.

JCO's Manuscript Processing System will benefit authors by

- eliminating the time and expense of copying and sending papers through the mail
- allowing authors to complete required submission forms quickly and easily online
- receiving nearly immediate acknowledgement of receipt of manuscripts
- tracking the status of manuscripts at any time online and
- accessing all reviews and decisions online.

Authors are encouraged to register at http://submit.jco.org.

For more details on *JCO*'s new online Manuscript Processing System, go online to http://www.jco.org/misc/announcements.shtml. Also, watch upcoming issues of *JCO* for updates like this one.

Downloaded from www.jco.org at National Cancer Center on May 6, 2005 .
Copyright © 2005 by the American Society of Clinical Oncology. All rights reserved.

[CANCER RESEARCH 64, 9101–9104, December 15, 2004]

Small In-Frame Deletion in the Epidermal Growth Factor Receptor as a Target for ZD6474

Tokuzo Arao,[1] Hisao Fukumoto,[1] Masayuki Takeda,[1] Tomohide Tamura,[2] Nagahiro Saijo,[2] and Kazuto Nishio[1,3]

[1]Shien-Lab, [2]Medical Oncology, National Cancer Center Hospital, Tsukiji, Japan; and [3]Pharmacology Division, National Cancer Center Research Institute, Tokyo, Japan

ABSTRACT

ZD6474 is an inhibitor of vascular endothelial growth factor receptor-2 (VEGFR-2/KDR) tyrosine kinase, with additional activity against epidermal growth factor receptor (EGFR) tyrosine kinase. ZD6474 inhibits angiogenesis and growth of a wide range of tumor models *in vivo*. Gefitinib ("Iressa") is a selective EGFR tyrosine kinase inhibitor that blocks signal transduction pathways implicated in cancer cell proliferation. Here, the ability of gefitinib and ZD6474 to inhibit tumor cell proliferation was examined directly in eight cancer cell lines *in vitro*, and a strong correlation was noted between the IC_{50} values of gefitinib and ZD6474 ($r = 0.79$). No correlation was observed between the sensitivity to ZD6474 and the level of EGFR or VEGFR expression. The NSCLC cell line PC-9 was seen to be hypersensitive to gefitinib and ZD6474, and a small (15-bp) in-frame deletion of an ATP-binding site (exon 19) in the EGFR was detected (delE746-A750–type deletion). To clarify the involvement of the deletional mutation of EGFR in the cellular sensitivity to ZD6474, we examined the effect of this agent on HEK293 stable transfectants expressing deletional EGFR that designed as the same deletion site observed in PC-9 cells (293-pΔ15). These cells exhibited a 60-fold higher sensitivity to ZD6474 compared with transfectants expressing wild-type EGFR. ZD6474 inhibited the phosphorylation of the mutant EGFR by 10-fold compared with cells with wild-type EGFR. In conclusion, the findings suggested that a small in-frame deletion in the EGFR increased the cellular sensitivity to ZD6474.

INTRODUCTION

Gefitinib ("Iressa") is an orally active, selective EGFR-tyrosine kinase inhibitor that blocks the signal transduction pathways implicated in the proliferation and survival of cancer cells and other host-dependent processes promoting cancer cell growth (1–3). Mutation of the EGFR tyrosine kinase in human non–small-cell lung carcinoma (NSCLC) and hyperresponsiveness to gefitinib in patients with NSCLC with this mutation recently were reported (4, 5). The mutations were small, in-frame deletions or substitutions clustered around the ATP-binding site in exons 18, 19, and 21 of the EGFR. The mutant receptors were significantly more sensitive to gefitinib than the wild-type receptor (IC_{50} 0.015 versus 0.1 μmol/L). However, of the 95 other primary tumors and 108 cell lines derived from other tumor types studied, none showed any mutations of this receptor (4). Conversely, Ohm *et al.* (6) reported that all four patients with gefitinib-responsive NSCLC were shown to have mutations of the EGFR near the ATP-binding site compared with none of seven cases showing no response to this drug. These results clearly suggest that the EGFR mutation may be a strong determinant of the tumor response to gefitinib.

ZD6474 is an inhibitor of VEGFR-2 and EGFR signaling that inhibits angiogenesis and tumor growth in a diverse range of tumor models (7). We previously have shown that the NSCLC cell line PC-9 is hypersensitive to gefitinib, with an IC_{50} value of ~0.02 μmol/L (8, 9). It subsequently was established that the PC-9 cells also showed hypersensitivity to ZD6474.

In this report, we discuss the presence of an EGFR deletional mutation and its ability to determine sensitivity to ZD6474.

MATERIALS AND METHODS

Reagents. ZD6474 and gefitinib (Iressa) were provided by AstraZeneca (Cheshire, United Kingdom).

Cell Culture. The human NSCLC cell lines PC-9 and PC-14 were established at the Tokyo Medical University (10, 11). The human epidermal carcinoma cell line A431, breast carcinoma cell line SK-BR-3, ovarian carcinoma cell line SK-OV-3, and colon carcinoma cell lines WiDr and LoVo were obtained from the American Type Culture Collection (Manassas, VA). The SBC-3 cells were supplied by Okayama University School of Medicine. All of the cell lines were maintained in Roswell Park Memorial Institute 1640 medium (Sigma, St. Louis, MO) supplemented with 10% heat-inactivated fetal bovine serum (FBS; Life Technologies, Rockville, MD), except for the LoVo (F12; Nissui Pharmaceutical, Tokyo, Japan), WiDr (modified Eagle's medium; Nissui Pharmaceutical), and A431 cells (Dulbecco's modified Eagle's medium; Nissui Pharmaceutical). The HEK293 cell line was obtained from the American Type Culture Collection and cultured in Dulbecco's modified Eagle's medium supplemented with 10% FBS.

***In vitro* Growth-Inhibition Assay.** The cell growth-inhibitory effect of gefitinib and ZD6474 was determined using the thiazolyl blue tetrazolium bromide (MTT) assay (Sigma). Briefly, 180 μL/well of the cell suspension were seeded onto Sumilon 96-well microculture plates (Sumitomo Bakelite, Akita, Japan) and incubated in 10% FBS-containing medium for 24 hours. The cells were treated with gefitinib or ZD6474 at various concentrations (4 nmol/L to 80 μmol/L) and cultured at 37°C in a humidified atmosphere for 72 hours. After the culture period, 20 μL of MTT reagent were added, and the plates were further incubated for 4 hours. After centrifugation of the plates, the culture medium was discarded, and wells were filled with dimethyl-sulfoxide. The absorbance of the cultures was measured at 562 nm using Delta-soft on a Macintosh computer (Apple, Cupertino, CA) interfaced to a Bio-Tek Microplate Reader EL-340 (BioMetallics, Princeton, NJ). This experiment was conducted in triplicate. The statistical analysis was performed using KaleidaGraph (Synergy Software, Reading, PA).

Plasmid Construction and Transfection. Construction of expression plasmid vector of mock (empty vector), wild-type EGFR, and the 15-bp deletional EGFR (delE746-A750 type deletion; ref. 4) that possess the same deletion site observed in PC-9 cells (Fig. 2A) in detail was described in another paper.[1] The plasmids were transfected into the HEK293 cells, and the transfectants were selected by Zeosin (Sigma). The stable transfectants (pooled cultures) of the empty vector, wild-type EGFR, and its deletion mutant were designated as Mock, 293-pEGFR, and 293-pΔ15, respectively.

Immunoblot Analysis. Immunoblot analysis was performed as described previously (3). EGFR antibody was purchased from Santa Cruz Biotechnology (no. 1005; Santa Cruz, CA) and Cell Signaling (Beverly, MA). Phospho-EGFR antibody (specific for Tyr-1068), human epidermal growth factor receptor 2, p44/p42 mitogen-activated protein kinase (MAPK), phospho-p44/p42 MAPK, AKT, phospho-AKT, and antirabbit horseradish peroxidase conjugated antibody all were purchased from Cell Signaling. The transfected cells cultured in

Received 7/1/04; revised 9/10/04; accepted 10/14/04.

Grant support: Funds for the 2nd Term Comprehensive 10 Year Strategy for Cancer Control and a Grant-in-Aid for Scientific Research from the Ministry of Education, Culture, Sports, Science and Technology of Japan (12217165). T. Arao is the Recipient of a Research Resident Fellowship from the Foundation of Promotion of Cancer Research in Japan.

The costs of publication of this article were defrayed in part by the payment of page charges. This article must therefore be hereby marked "*advertisement*" in accordance with 18 U.S.C. Section 1734 solely to indicate this fact.

Requests for reprints: Shien-Lab, Medical Oncology, National Cancer Center Hospital, Tsukiji 5-1-1, Chuo-ku, Tokyo 104-0045, Japan. Phone: 81-3-3542-2511; Fax: 81-3-3542-5185; E-mail: kmishio@gan2.res.ncc.go.jp.

©2004 American Association for Cancer Research.

[1] Unpublished observation.

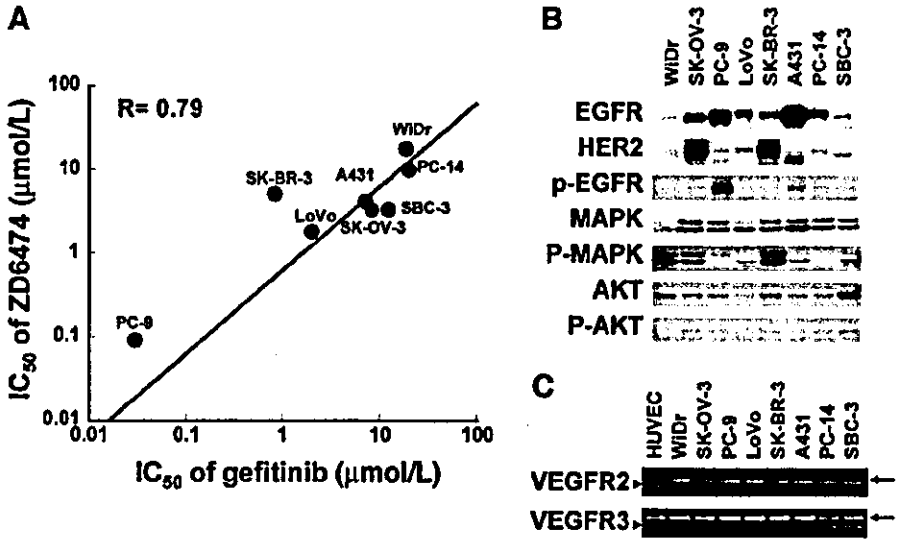

Fig. 1. The cellular characteristics and growth-inhibitory effect of gefitinib and ZD6474. *A*, correlation plot of the IC_{50} values of gefitinib and ZD6474 in human cancer cell lines. The growth-inhibitory effect against PC-9, WiDr, LoVo, PC-14, A431, SK-OV-3, SK-BR-3, and SBC-3 cells was determined by MTT assay (72-hour exposure). The data were obtained from three independent experiments. *B*, expression and phosphorylation status of EGFR and downstream molecules in human cancer cell lines. Data were obtained by immunoblot analysis with anti-EGFR, anti-phospho-EGFR, anti-HER2, anti-phospho-p44/p42 MAPK, anti-p44/p42 MAPK, anti-AKT, anti-phospho-AKT, and anti-AKT. *C*, The mRNA expression level of VEGFR-2 and VEGFR-3 was determined by reverse transcription-PCR. Human umbilical vascular endothelial cell (*HUVEC*) was used as the positive control. Whereas VEGFR-2 expression was not detected in any of the cancer cell lines, VEGFR-3 expression was detected in the PC-14 and SBC-3 cells; *arrows*, β-actin; *arrowheads*, VEGFR-2 or VEGFR-3.

the serum-free medium for 24 hours were stimulated by the addition of EGF (Sigma) at a final concentration of 10 ng/mL. After a 30-minute incubation, the cells were incubated for an additional 3 hours in the presence of ZD6474 and then collected for immunoblot analysis. The subconfluent cancer cell lines were cultured in medium containing 10% FBS and collected for immunoblot analysis.

Reverse-Transcription PCR. Five micrograms of total RNA from each cultured cell line were converted to cDNA using a GeneAmp RNA-PCR kit (Applied Biosystems, Foster City, CA). The primers used for the PCR were as follows: VEGFR-2, 5′-CAGACGGACAGTGGTATGGTTC-3′ (forward) and 5′-ACCTGCTGGTGGAAAGAACAAC-3′ (reverse); and VEGFR-3, 5′-AGCCATTCATCAACAAGCCT-3′ (forward) and 5′-GGCAACAGCTG-GATGTCATA-3′ (reverse). As a control, the following human β-actin primers were used: 5′-GGAAATCGTGCGTGACATT-3′ and 5′-CATCTGCTG-GAAGGTGGACAG-3′. PCR amplification consisted of 35 cycles (95°C for 45 seconds, 62°C for 45 seconds, and 72°C for 60 seconds) followed by incubation at 72°C for 7 minutes. The bands were visualized by ethidium bromide staining.

Sequencing. Sequencing of exons 18 through 21 of EGFR cDNA in the tumor cell lines was performed. The cDNAs were amplified using the following primers: 5′-TCCAAACTGCACCTACGGATGC-3′ (forward) and 5′-CATCAACTCCCAAACGGTCACC-3′ (reverse). PCR amplification consisted of 25 cycles (95°C for 45 seconds, 55°C for 30 seconds, and 72°C for 60 seconds). The sequences of the PCR products were determined using ABI prism 310 (Applied Biosystems). Amplification and sequencing were performed in duplicate for each tumor cell line. The sequences were compared with the GenBank-archived human sequence of EGFR (accession no. NM_005228.3).

RESULTS

Growth-Inhibitory Activity of Gefitinib and ZD6474. We examined the *in vitro* growth-inhibitory activities of gefitinib and ZD6474 on eight cancer cell lines by MTT assay. The IC_{50} values of gefitinib and ZD6474 for each cell line were compared and plotted as shown in Fig. 1*A*. Good correlation ($r = 0.79$) was observed between the IC_{50} values of gefitinib and ZD6474, suggesting that the mechanisms underlying the growth-inhibitory activities of the two drugs *in vitro* might be similar. To clarify the correlation between the cellular sensitivity for gefitinib and ZD6474 and the EGFR status, we examined the expression and phosphorylation levels of EGFR in the cell lines by immunoblot analysis (Fig. 1*B*). No correlation was found between the expression status or the phosphorylation level of EGFR and the IC_{50} value of either drug. There also was no correlation between the cellular sensitivity and the phosphorylation status of any downstream molecules, such as phosphorylated MAPK and phospho-AKT (Fig. 1*B*). To determine the correlation between the VEGFR expression levels and cellular sensitivity, we examined the mRNA levels of the VEGFR-2 and VEGFR-3 in the cell lines by reverse transcription-PCR and detected VEGFR-3 transcripts in PC-14 and SBC-3 cells (Fig. 1*C*). VEGFR-2 was not detectable in all of the cancer cell lines. The results suggested that there was no correlation between the cellular sensitivity to ZD6474 and the VEGFR-2 and VEGFR-3 expression level. Among all of the cell lines examined, the PC-9 cell line was found to be hypersensitive to gefitinib (IC_{50} = 0.03 ± 0.002 μmol/L) and ZD6474 (IC_{50} values = 0.09 ± 0.01 μmol/L). The respective IC_{50} values of gefitinib and ZD6474 for the other cell lines were as follows: WiDr, 18.7 ± 2.5 μmol/L and 17.7 ± 2.3 μmol/L; SK-OV-3, 8.3 ± 1.5 μmol/L and 3.3 ± 0.2 μmol/L; LoVo, 2.0 ± 0.3 μmol/L and 1.8 ± 0.2 μmol/L; A431, 7.1 ± 0.9 μmol/L and 4.1 ± 0.2 μmol/L; PC-14, 20 ± 2.1 μmol/L and 10 ± 1.2 μmol/L; SK-BR-3, 0.8 ± 0.15 μmol/L and 5.2 ± 0.1 μmol/L; and SBC-3, 12.3 ± 2.1 μmol/L and 3.3 ± 0.3 μmol/L.

Fifteen-Base Pair In-Frame Deletion of EGFR in PC-9 Cells. To determine the cellular determinants of the hypersensitivity of the PC-9 cells to gefitinib, we determined the sequence of the EGFR mRNA in the PC-9 cells. The analysis revealed a 15-bp in-frame deletion around the ATP-binding site in exon 19 (Fig. 2*A*). No deletion or mutation was found in the other cell lines. The 15-bp in-frame deletion in the EGFR was consistent with the observations of Ohm *et al.* (6) in four patients with lung cancer.

Deletional Mutation of EGFR Increases the Cellular Sensitivity to ZD6474. We hypothesized that the cellular hypersensitivity of the PC-9 cells to ZD6474 was attributable to the deletional mutation of EGFR in these cells. To confirm the validity of this hypothesis, we examined ZD6474 sensitivity to HEK293 transfectant expressing the 15-bp deletion mutant EGFR or wild-type EGFR. The sequencing of EGFR cDNA obtained from 293-pEGFR and 293-pΔ15 cells was shown (Fig. 2*B*). The sensitivity of the transfectants was examined by 72-hour exposure of ZD6474 using MTT assay. The 293-pΔ15 cells were found to be 60-fold more sensitive to ZD6474 than the mock and wild-type EGFR transfectants (Fig. 3*A*). The IC_{50} of ZD6474 for the 293-pΔ15 cells, 293-pEGFR cells, and the mock transfectants were 0.08, 5.2, and 6.3 μmol/L, respectively.

The EGFR expression levels in the transfectants were quantified by immunoblot analysis using anti-EGFR antibody recognizing the

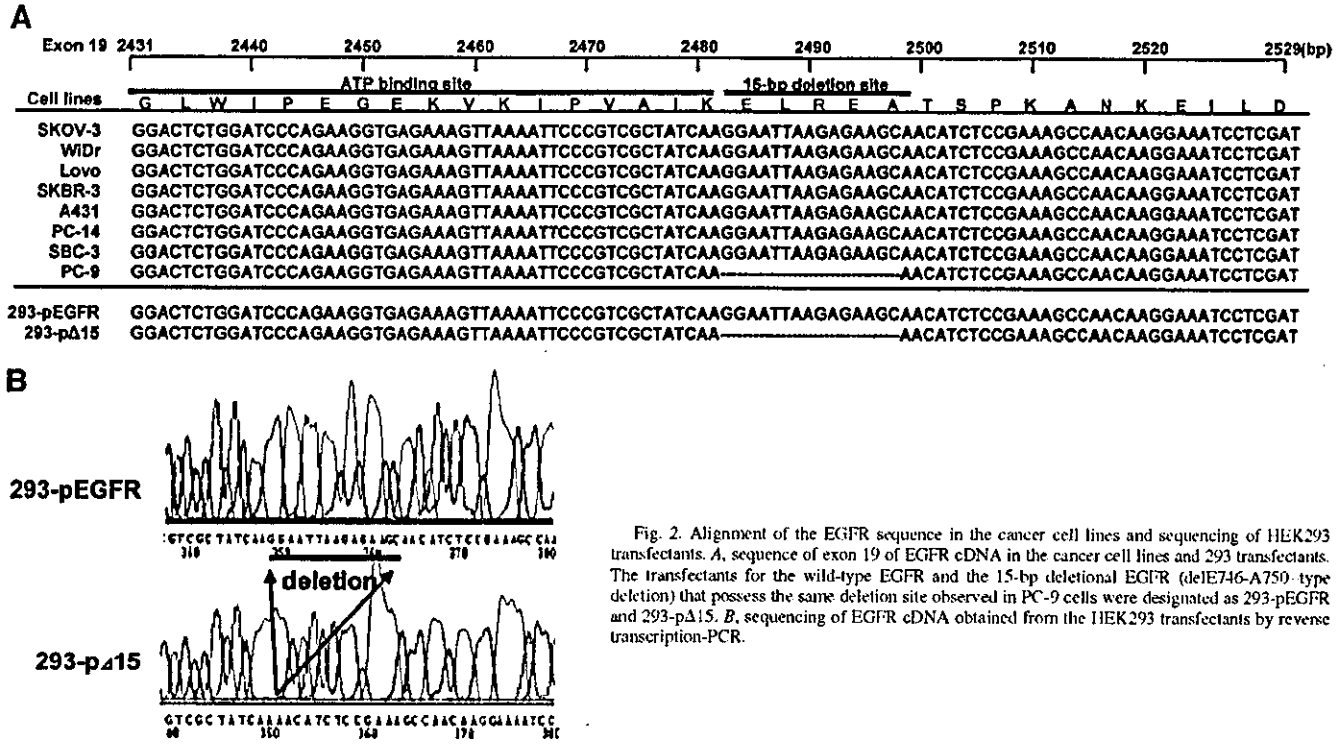

Fig. 2. Alignment of the EGFR sequence in the cancer cell lines and sequencing of HEK293 transfectants. *A*, sequence of exon 19 of EGFR cDNA in the cancer cell lines and 293 transfectants. The transfectants for the wild-type EGFR and the 15-bp deletional EGFR (delE746-A750 type deletion) that possess the same deletion site observed in PC-9 cells were designated as 293-pEGFR and 293-pΔ15. *B*, sequencing of EGFR cDNA obtained from the HEK293 transfectants by reverse transcription-PCR.

COOH-terminus of EGFR. High expression of EGFR proteins was detected in the 293-pΔ15 cells and 293-pEGFR cells but not in the mock cells (Fig. 3*B*). Exposure to ZD6474 did not affect the expression of levels of either the wild-type or the mutant EGFR. EGFR status was quantified by measuring the phosphorylation level of the Tyr-1068 residue, commonly used as a marker of the autophosphorylation of EGFR (12).

Under the condition of serum starvation, wild-type EGFR did not show any autophosphorylation, whereas the addition of EGF activated the receptor. However, marked autophosphorylation of the mutant EGFR was observed, even without the addition of EGF (Fig. 3*B*). ZD6474 exposure inhibited the phosphorylation of wild-type EGFR and mutant EGFR in a dose-dependent manner, with 2 μmol/L and 0.2 μmol/L of ZD6474 completely inhibiting phosphorylation of the wild-type EGFR and mutant EGFR, respectively. These results suggest that cells expressing the deletion mutant of EGFR are markedly more sensitive to the inhibitory effect of ZD6474 than those expressing wild-type EGFR.

DISCUSSION

Recent reports by Paez and Lynch have indicated that deletional mutations of EGFR impact on the therapeutic effects of the molecular-

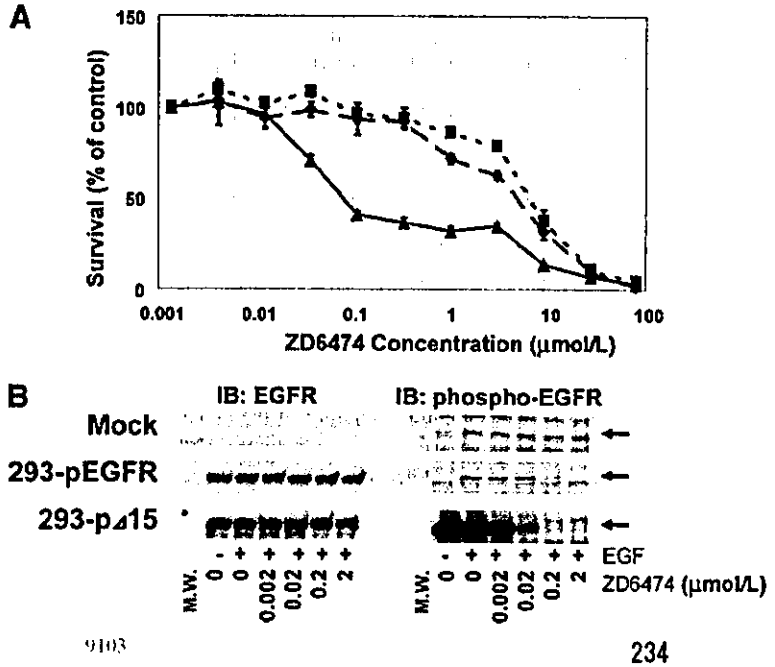

Fig. 3. Effect of ZD6474 on cellular growth inhibition and phosphorylated status of EGFR in the HEK293 transfectants. *A*, The cellular sensitivity of the transfectants against ZD6474 was determined by MTT assay (72-hour exposure). The mean values and SD represent the values obtained from the growth-inhibition curves in three independent experiments. ♦, mock (empty vector); ■, 293-pEGFR (wild-type EGFR); ▲, 293-pΔ15 (deletional-mutant EGFR). *B*, effect of EGF stimulation and ZD6474 exposure on mock, wild-type EGFR, and deletional mutant EGFR-transfected HEK293 cells determined by immunoblot analysis. Cells cultured under serum starvation for 24 hours were exposed to 10 ng/ml. EGF for 30 minutes and then treated with 0.002 to 2 μmol/L ZD6474 for 3 hours in the presence or absence of EGF. *Left*, EGFR expression levels, *right*, EGFR phosphorylation levels

targeted EGFR inhibitor gefitinib (4, 5). Here, we show that a 15-bp deletional mutation residing near the ATP binding site of EGFR in cancer cells also increases the sensitivity of the cells to ZD6474.

ZD6474 is a small molecule inhibitor of VEGFR-2 tyrosine kinase that is in Phase II clinical evaluation. *In vivo*, this compound inhibits VEGF signaling, tumor-induced angiogenesis, and the growth of a histologically diverse panel of tumor xenografts. This includes highly significant activity against tumor xenografts with intrinsic or acquired resistance to EGFR inhibitors (13). However, ZD6474 also has activity against EGFR tyrosine kinase that may give additional therapeutic benefit when tumors have a high dependency on EGFR signaling for growth and/or survival. This has been shown in PC-9 cells that are hypersensitive to treatment with gefitinib (9). PC-9 tumor cells also are hypersensitive to ZD6474 *in vitro* and regress in response to ZD6474 treatment when grown as tumor xenografts *in vivo* (14).

We have shown that PC-9 cells contain a 15-bp in-frame deletional mutation in EGFR, and this mutation may confer increased sensitivity to ZD6474 and gefitinib. The difference in ZD6474 concentration required for complete inhibition of wild-type and mutant EGFR phosphorylation was relatively small (2 versus 0.2 μmol/L), whereas difference in sensitivity to ZD6474 was large (60-fold).

The deletional EGFR was constitutively phosphorylated, and the addition of EGF to the cultures did not result in any additional increase in phosphorylation (Fig. 3*B*). These observations contradict data reported by Lynch *et al.* (4), who showed that a receptor with a similar deletion was still regulated by EGF.

The most possible explanation for this contradiction is that the expression level of deletional EGFR in the 293-pΔ15 cells is much higher than that of the transient transfectant of Del L747-P753insS reported by Lynch *et al.* Ligand-independent oligomerization of the receptor and phosphorylation may have occurred in the 293-pΔ15 cells as a result. This hypothesis is consistent with the result that PC-9 cells harboring the same 15-bp deletion showed a stronger phosphorylation of the EGFR in a 10% FBS medium than other nonhypersensitive cell lines (Fig. 1*B*).

The other possible explanation is that apparent distinct amino acid sequences of EGFR exist between our mutant and that of Lynch *et al.* (293-pΔ15, VAIKELREATSPK>VAIKTSPK; delL747-P753insS, VAIKELREATSPK>VAIKESK). Five amino acids are simply deleted in the 293-pΔ15 cells, whereas six amino acids are deleted and serine is inserted in the delL747-P753insS cells. This small difference may be critical to the ATP-binding properties of 293-pΔ15 and delL747-P753insS, determining whether EGFR is constitutively active. Therefore, it is not surprising that our constitutive active form of EGFR is out of ligand regulation.

The mock-transfected 293 cells and 293-pEGFR cells were not sensitive to the growth-inhibitory effect of ZD6474 (Fig. 3*A*), indicating that these cells were independent of EGFR signaling. The 293 cells are oncogenic transformant. Therefore, the 293 cells were considered to have acquired the dependency on the oncogenic signal. Conversely, the overexpression of the deletional EGFR transduces the excess signal to downstream of EGFR in the 293-pΔ15 cells. If the downstream mutant EGFR signaling pathway were shared with that of the oncogenic signaling pathway in the cells, the excess and constitutive signal from the mutant EGFR would dominate the downstream pathway, possibly influencing the dependency of the cells on the EGFR signal.

A recent report by Sordella *et al.* (15) showed the mutant EGFRs (del L747-P753insS and L858R) expressing a stable transfectant selectively activate AKT and STAT signaling pathways. They also showed that NSCLC cell lines that harboring mutant EGFR transduce survival signals and depend on the acquisition of these signals. Their evidence is consistent with our present speculations. We now are investigating the downstream pathways of the mutant EGFR signaling in the 293-pΔ15 cells.

In summary, inhibition of VEGFR-2 tyrosine kinase by ZD6474 may potentially confer activity against tumors that are not dependent on EGFR signaling. Nevertheless, the additional activity of ZD6474 against EGFR tyrosine kinase could provide further benefit, particularly when EGFR is mutated. Patients with lung adenocarcinoma showing EGFR mutations are likely to be highly sensitive to gefitinib and ZD6474 treatment.

REFERENCES

1. Ciardiello F, Caputo R, Tortora G, et al. Antitumor effect and potentiation of cytotoxic drugs activity in human cancer cells by ZD-1839 (Iressa), an epidermal growth factor receptor-selective tyrosine kinase inhibitor. Clin Cancer Res 2000;6: 2053–63.
2. Moasser MM, Basso A, Averbuch SD, Rosen N. The tyrosine kinase inhibitor ZD1839 ("Iressa") inhibits HER2-driven signaling and suppresses the growth of HER2-overexpressing tumor cells. Cancer Res 2001;61:7184–8.
3. Koizumi F, Kanzawa F, Nishio K, et al. Synergistic interaction between the EGFR tyrosine kinase inhibitor gefitinib ("Iressa") and the DNA topoisomerase I inhibitor CPT-11 (irinotecan) in human colorectal cancer cells. Int J Cancer 2004;108:464–72.
4. Lynch TJ, Bell DW, Haber DA, et al. Activating mutations in the epidermal growth factor receptor underlying responsiveness of non-small-cell lung cancer to gefitinib. N Engl J Med 2004;350:2129–39.
5. Paez JG, Janne PA, Meyerson M, et al. EGFR mutations in lung cancer: correlation with clinical response to gefitinib therapy. Science 2004;304:1497–500.
6. Ohm JE, Amann JM, Carbone DP. Acquired EGFr TKI resistance associated with mutation of the EGFr. Presented at the 95th Annual Meeting of the American Association of Cancer Research, November 17–21, 2004, Bonita Springs, FL.
7. Ciardiello F, Caputo R, Tortora G, et al. Antitumor effects of ZD6474, a small molecule vascular endothelial growth factor receptor tyrosine kinase inhibitor, with additional activity against epidermal growth factor receptor tyrosine kinase. Clin Cancer Res 2003;9:1546–56.
8. Naruse I, Ohmori T, Nishio K, et al. Antitumor activity of the selective epidermal growth factor receptor-tyrosine kinase inhibitor (EGFR-TKI) Iressa (ZD1839) in an EGFR-expressing multidrug-resistant cell line in vitro and in vivo. Int J Cancer 2002;98:310–5.
9. Koizumi F, Taguchi F, Shimoyama T, Saijo N, Nishio K. Mechanism of resistance to epidermal growth factor receptor inhibitor ZD1839: a role for inhibiting phosphorylation of EGFR at Tyr1068. Presented at the 94th Annual Meeting of the American Association of Cancer Research, July 11–14, 2003, Washington, DC.
10. Kawamura-Akiyama Y, Kusaba H, Nishio K, et al. Non-cross resistance of ZD0473 in acquired cisplatin-resistant lung cancer cell lines. Lung Cancer 2002;38:43–50.
11. Nishio K, Arioka H, Saijo N, et al. Enhanced interaction between tubulin and microtubule-associated protein 2 via inhibition of MAP kinase and CDC2 kinase by paclitaxel. Int J Cancer 1995;63:688–93.
12. Nielsen UB, Cardone MH, Sinskey AJ, MacBeath G, Sorger PK. Profiling receptor tyrosine kinase activation by using Ab microarrays. Proc Natl Acad Sci USA 2003;100:9330–5.
13. Ciardiello F, Bianco R, Tortora G, et al. Antitumor activity of ZD6474, a vascular endothelial growth factor receptor tyrosine kinase inhibitor, in human cancer cells with acquired resistance to antiepidermal growth factor receptor therapy. Clin Cancer Res 2004;10:784–93.
14. Taguchi F, Koh Y, Nishio K, et al. Anticancer effects of ZD6474, a VEGF receptor tyrosine kinase inhibitor, in gefitinib (Iressa) sensitive and resistant xenograft models. Cancer Sci 2004;in press.
15. Sordella R, Bell DW, Haber DA, Settleman J. Gefitinib-sensitizing EGFR mutations in lung cancer activate anti-apoptotic pathways. Science 2004;305:1163–7.

Anticancer effects of ZD6474, a VEGF receptor tyrosine kinase inhibitor, in gefitinib ("Iressa")-sensitive and resistant xenograft models

Fumiko Taguchi,[1] Yasuhiro Koh,[1] Fumiaki Koizumi,[1,2] Tomohide Tamura,[3] Nagahiro Saijo[3] and Kazuto Nishio[1,2,4]

[1]Pharmacology Division, National Cancer Center Research Institute; and [2]Shien-Lab and [3]Medical Oncology, National Cancer Center Hospital, 5-1-1 Tsukiji, Chuo-ku, Tokyo 104-0045

(Received August 6, 2004/Revised September 27, 2004/Accepted October 8, 2004)

ZD6474 is a novel, orally available inhibitor of vascular endothelial growth factor (VEGF) receptor-2 (KDR) tyrosine kinase, with additional activity against epidermal growth factor receptor (EGFR) tyrosine kinase. ZD6474 has been shown to inhibit angiogenesis and tumor growth in a range of tumor models. Gefitinib ("Iressa") is an selective EGFR tyrosine kinase inhibitor (TKI) that blocks signal transduction pathways. We examined the antitumor activity of ZD6474 in the gefitinib-sensitive lung adenocarcinoma cell line, PC-9, and a gefitinib-resistant variant (PC-9/ZD). PC-9/ZD cells showed cross-resistance to ZD6474 in an *in vitro* dye formation assay. In addition, ZD6474 showed dose-dependent inhibition of EGFR phosphorylation in PC-9 cells, but inhibition was only partial in PC-9/ZD cells. ZD6474-mediated inhibition of tyrosine residue phosphorylation (Tyr992 and Tyr1045) on EGFR was greater in PC-9 cells than in PC-9/ZD cells. These findings suggest that the inhibition of EGFR phosphorylation by ZD6474 can contribute a significant, direct growth-inhibitory effect in tumor cell lines dependent on EGFR signaling for growth and/or survival. The effect of ZD6474 (12.5–50 mg/kg/day p.o. for 21 days) on the growth of PC-9 and PC-9/ZD tumor xenografts in athymic mice was also investigated. The greatest effect was seen in gefitinib-sensitive PC-9 tumors, where ZD6474 treatment (>12.5 mg/kg/day) resulted in tumor regression. Dose-dependent growth inhibition, but not tumor regression, was seen in ZD6474-treated PC-9/ZD tumors. These studies demonstrate that the additional EGFR TKI activity may contribute significantly to the antitumor efficacy of ZD6474, in particular in those tumors that are dependent on continued EGFR-signaling for proliferation or survival. In addition, these results provide a preclinical rationale for further investigation of ZD6474 as a potential treatment option for both EGFR-TKI-sensitive and EGFR-TKI-resistant tumors. (Cancer Sci 2004; 95: 984–989)

ZD6474 is a novel, orally available inhibitor of VEGF receptor-2 (KDR) tyrosine kinase, with additional activity against EGFR tyrosine kinase, and it inhibits angiogenesis and tumor growth in a diverse range of tumor models.[1,2] Phase I clinical evaluation has shown ZD6474 to be generally well tolerated, and tumor responses in patients with non-small cell lung cancer (NSCLC) have been documented.[3,4] Thus, ZD6474 is considered to be a multi-target tyrosine kinase inhibitor active against solid tumors. The purpose of this study is to clarify the mode of antitumor action of ZD6474 as compared with that of gefitinib ("Iressa," ZD1839). Gefitinib is an orally active, selective EGFR tyrosine kinase inhibitor (EGFR-TKI) that blocks signal transduction pathways implicated in the proliferation and survival of cancer cells and other host-dependent processes promoting tumor growth.[5–7] Gefitinib is now available clinically for non-small cell lung cancer patients. In order to elucidate the mode of action of ZD6474, the antitumor activity and pharmacodynamics were investigated in an established human lung cancer cell line resistant to gefitinib (PC-9/ZD cells).[8] This approach allowed us to clarify the common and differential modes of actions of gefitinib and ZD6474 in lung cancer, and this will be important for deciding how to use ZD6474 in non-small cell lung cancer patients in combination with gefitinib.

Materials and Methods

Reagents and cell culture. ZD6474 and gefitinib ("Iressa," ZD1839) were provided by AstraZeneca (Macclesfield, UK). Human NSCLC cell lines PC-9 and PC-14 were used.[9,10] In addition, a gefitinib-resistant subline, PC-9/ZD, was derived from PC-9 cells by short-term exposure to the mutagen *N*-methyl-*N'*-nitro-*N*-nitrosoguanidine, continuous exposure to 0.2–0.5 μ*M* gefitinib for 28 days, and subcloning. The resistant phenotype has been stable for at least 6 months under drug-free conditions.[8] The PC-9/ZD cell line shows no cross-resistance to conventional anticancer drugs.[8] Cells were maintained in RPMI-1640 (Sigma Chemical Co., St. Louis, MO) supplemented with 10% heat-inactivated fetal bovine serum (Gibco BRL, Grand Island, NY).

Antibodies. Anti-vonWillebrand Factor (vWF) antibody was purchased from Chemicon, Temecula, CA. Affinity-purified antibody to EGFR was purchased from Santa Cruz, CA and affinity-purified antibodies to phospho-EGFR specific for Tyr845, Tyr992, Tyr1045, and Tyr1068 were purchased from Cell Signaling Technology, Beverly, MA.

Growth inhibition assay. Cell sensitivity to ZD6474 and gefitinib was estimated by means of the 3-(4,5-dimethylthiazol-2-yl)-2,5-diphenyltetrazolium bromide (MTT) assay as described previously.[11] Briefly, PC-9, PC-9/ZD, or PC-14 cells were exposed to 0–10 μ*M* ZD6474 or gefitinib for 72 h before measuring absorbance. Optical density was assessed at 562–630 nm using an EL340 96-well microtiter plate reader (Bio-Tek, Winooski, VT).

Xenograft studies in athymic mice. Suspensions of PC-9 cells (5×10^6) or PC-9/ZD cells (3×10^6) were injected subcutaneously into the backs of 5-week-old female athymic mice (Japan Charles River Co., Atsugi, Japan). After 1 week (tumors >95 mm^3), mice were randomly allocated into groups of six animals to receive ZD6474 (12.5, 25, or 50 mg/kg/day), gefitinib (12.5, 25, or 50 mg/kg/day) or vehicle only by oral gavage. Tumor diameter and body weight were measured twice weekly. The tumor volume was calculated (width^2×length/2) and is presented as a percentage of the pretreatment value. A tumor volume below 100% of the pretreatment volume was defined as "tumor reduction." Experiments were performed in accordance with the UK Coordinating Committee on Cancer Research Guidelines for the welfare of animals in experimental neoplasia (second edition). After 3 weeks of treatment, tumors were removed.

[4]To whom correspondence should be addressed.
E-mail: knishio@gan2.res.ncc.go.jp

Abbreviations: VEGF, vascular endothelial growth factor; EGFR, epidermal growth factor receptor; TKI, tyrosine kinase inhibitor; NSCLC, non-small cell lung cancer; MTT, 3-(4,5-dimethylthiazol-2-yl)-2,5-diphenyltetrazolium bromide.